

Fig. 4. CD81 is expressed at high levels in granulosa cells during oogenesis. Frozen sections of ovaries from wild-type mice were stained with anti-mouse CD81 mAb and with anti-ZP3 mAb. DIC represents a photograph taken by differential interference contrast. Scale bar, 20 μ m. [See color version online at www.interscience.wiley.com.]

DISCUSSION

CD81 has been suggested to be a protein playing a role in membrane fusion events, but the function of CD81 in sperm-egg fusion remains unknown. As suggested by Rubinstein et al. (2006), CD9 and CD81 may have different roles in sperm-egg fusion. This notion is supported by the following facts: (1) deletion of a single gene, CD9 or CD81, causes impaired fertilization, and the expression of CD9 on eggs is not perturbed by CD81 deficiency, and (2) CD9^{-/-} eggs injected with mRNA encoding CD81 cannot be fully rescued to the same degree as those injected with CD9 mRNA (Kaji et al., 2002).

Generally, the acrosome reaction is a change in the membrane of sperm that are activated for penetration into zona pellucida and facilitates the subsequent fusion with the egg membrane (Baba et al., 1994). During the acrosome reaction, the disruption of the acrosome covering the sperm head causes the release of acrosin and other proteolytic substances. As previously reported (Moreno and Alvarado, 2006), these materials included in the acrosome are important for the penetration of sperm into the zona pellucida and for sperm-egg fusion, but the molecular mechanism underlying the acrosome reaction is largely unknown. When wild-type eggs were incubated with sperm expressing EGFP in the acrosomes, we found the presence of acrosome-intact

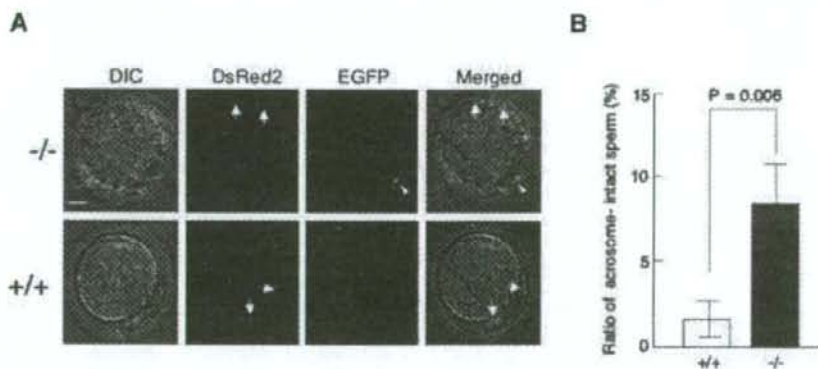


Fig. 5. In vitro fertilization assay for acrosome reaction. **A:** Representative photographs. CD81^{-/-} eggs were incubated with transgenic sperm expressing EGFP at acrosomes in the sperm heads. Eggs from wild-type females were also subjected to fertilization using the AR-GFP transgenic sperm as controls. Four hours after insemination, the eggs were inspected for fluorescence using a confocal microscope. As shown in the upper panel, some CD81^{-/-} eggs had sperm with green fluorescence (indicated by arrowheads) in their head region in the perivitelline space, while almost no wild-type eggs had such types of sperm (lower panel). Photomicrographs taken under light (DIC); photomicrographs taken for detecting DsRed2 translocated to mitochondria by the retention signal (Mt-DsRed2) and specifically expressed in the mid-piece of sperm (indicated by arrows); photomicrographs taken for detecting EGFP-derived green fluorescence specifically expressed in the head region of sperm (indicated by arrowheads);

merged images. Scale bar, 20 μ m. **B:** Examination of acrosome reaction using EGFP-expressing sperm. CD81^{-/-} or wild-type eggs were fertilized in vitro with epididymal sperm expressing EGFP in the acrosomes. Four hours after insemination, the sperm entering into the perivitelline space were inspected for fluorescence using a confocal microscope. Note that the number of sperm carrying intact acrosomes (exhibiting green fluorescence in the sperm head region, as shown in A) and entering into the perivitelline space of CD81^{-/-} eggs was significantly higher than that of acrosome-intact sperm entering into the perivitelline space of wild-type eggs. Acrosome-intact sperm can easily be detected since they exhibit bright green fluorescence in their head region. The total number of sperm entered into perivitelline space can be counted by inspection for red fluorescence in the mid-piece of the sperm. [See color version online at www.interscience.wiley.com.]

sperm in the outer layer of the zona pellucida (data not shown), but almost all sperm that penetrated into the perivitelline space had lost the acrosome caps (Fig. 5). These findings suggest that the acrosome reaction may occur in the perivitelline space and/or inner layer of the zona pellucida.

Another possible reason for the failure of the acrosome reaction of EGFP-expressing sperm in CD81^{-/-} eggs is that "zona hardening" in CD81^{-/-} eggs may not be sufficient compared to that in wild-type eggs. The weakened zona hardening might permit the penetration of some acrosome-intact sperm into CD81^{-/-} eggs. However, since proteins other than components forming the zona pellucida may be triggers for preventing polyspermy and zona hardening (Sun, 2003), it would be of interest to test whether CD81 and ZP3 interact with each other.

In conclusion, the results of our IVF experiments suggest the possible involvement of CD81 in the acrosome reaction of zona pellucida-penetrated sperm prior to the fusion of sperm with eggs. Extensive attempts to elucidate the role of CD81 in the acrosome reaction are now underway.

ACKNOWLEDGMENTS

We are thankful for Dr. Tsujimoto (Faculty of Medicine, Osaka University) for kindly providing mt-DsRed2 construct for transgenic production. This work was supported by a grant from Precursory Research for Embryonic Science and Technology (PRESTO), The Ministry of Health, Labour and Welfare, and a grant-in aid for Scientific Research, The Ministry of Education, Culture, Sports, and Technology, of Japan.

REFERENCES

- Baba T, Azuma S, Kashiwabara S, Toyoda Y. 1994. Sperm from mice carrying a targeted mutation of the acrosin gene can penetrate the oocyte zona pellucida and effect fertilization. *J Biol Chem* 269: 31845–31849.
- Beebe SJ, Leyton L, Burks D, Ishikawa M, Fuerst T, Dean J, Saling P. 1992. Recombinant mouse ZP3 inhibits sperm binding and induces the acrosome reaction. *Dev Biol* 151:48–54.
- Buccione R, Schroeder AC, Eppig JJ. 1990. Interactions between somatic cells and germ cells throughout mammalian oogenesis. *Biol Reprod* 43:543–547.
- Cormier EG, Tsamis F, Kajumo F, Durso RJ, Gardner JP, Dragic T. 2004. CD81 is an entry coreceptor for hepatitis C virus. *Proc Natl Acad Sci USA* 101:7270–7274.
- Deng J, Yeung VP, Tsitoura D, DeKruyff RH, Umetsu DT, Levy S. 2000. Allergen-induced airway hyperreactivity is diminished in CD81-deficient mice. *J Immunol* 165:5054–5061.
- Higginbottom A, Quinn ER, Kuo CC, Flint M, Wilson LH, Bianchi E, Nicosia A, Monk PN, McKeating JA, Levy S. 2000. Identification of amino acid residues in CD81 critical for interaction with hepatitis C virus envelope glycoprotein E2. *J Virol* 74:3642–3649.
- Kaji K, Oda S, Miyazaki S, Kudo A. 2002. Infertility of CD9-deficient mouse eggs is reversed by mouse CD9, human CD9, or mouse CD81; polyadenylated mRNA injection developed for molecular analysis of sperm-egg fusion. *Dev Biol* 247:327–334.
- Kaji K, Oda S, Shikano T, Ohnuki T, Uematsu Y, Sakagami J, Tada N, Miyazaki S, Kudo A. 2000. The gamete fusion process is defective in eggs of Cd9-deficient mice. *Nat Genet* 24:279–282.
- Le Naour F, Rubinstein E, Jasmin C, Prenant M, Boucheix C. 2000. Severely reduced female fertility in CD9-deficient mice. *Science* 287:319–321.
- Miyado K, Yamada G, Yamada S, Hanawa H, Nakamura Y, Ryu F, Suzuki K, Kosai K, Inoue K, Ogura A, Okabe M, Mekada E. 2000. Requirement of CD9 on the egg plasma membrane for fertilization. *Science* 287:321–324.
- Miyazaki T, Muller U, Campbell KS. 1997. Normal development but differentially altered proliferative responses of lymphocytes in mice lacking CD81. *EMBO J* 16:4217–4225.
- Moreno RD, Alvarado CP. 2006. The mammalian acrosome as a secretory lysosome: New and old evidence. *Mol Reprod Dev* 73:1430–1434.
- Nakanishi T, Ikawa M, Yamada S, Parvonen M, Baba T, Nishimune Y, Okabe M. 1999. Real-time observation of acrosomal dispersal from mouse sperm using GFP as a marker protein. *FEBS Lett* 449:277–283.
- Pileri P, Uematsu Y, Campagnoli S, Galli G, Falugi F, Petracca R, Weiner AJ, Houghton M, Rosa D, Grandi G, Abrignani S. 1998. Binding of hepatitis C virus to CD81. *Science* 282:938–941.
- Rubinstein E, Ziyat A, Prenant M, Wrobel E, Wolf JP, Levy S, Le Naour F, Boucheix C. 2006. Reduced fertility of female mice lacking CD81. *Dev Biol* 290:351–358.
- Schwander M, Leu M, Stumm M, Dorchiev OM, Ruegg UT, Schittny J, Muller U. 2003. Beta1 integrins regulate myoblast fusion and sarcomere assembly. *Dev Cell* 4:673–685.
- Sun QY. 2003. Cellular and molecular mechanisms leading to cortical reaction and polyspermy block in mammalian eggs. *Microsc Res Tech* 61:342–348.
- Tachibana I, Hemler ME. 1999. Role of transmembrane 4 superfamily (TM4SF) proteins CD9 and CD81 in muscle cell fusion and myotube maintenance. *J Cell Biol* 146:893–904.
- Takahashi Y, Bigler D, Ito Y, White JM. 2001. Sequence-specific interaction between the disintegrin domain of mouse ADAM 3 and murine eggs: Role of beta1 integrin-associated proteins CD9, CD81, and CD98. *Mol Biol Cell* 12:809–820.
- Takeda Y, Tachibana I, Miyado K, Kobayashi M, Miyazaki T, Funakoshi T, Kimura H, Yamane H, Saito Y, Goto H, Yoneda T, Yoshida M, Kumagai T, Osaki T, Hayashi S, Kawase I, Mekada E. 2003. Tetraspanins CD9 and CD81 function to prevent the fusion of mononuclear phagocytes. *J Cell Biol* 161:945–956.
- Yamagata K, Nakanishi T, Ikawa M, Yamaguchi R, Moss SB, Okabe M. 2002. Sperm from the calmodulin-deficient mouse have normal abilities for binding and fusion to the egg plasma membrane. *Dev Biol* 250:348–357.



Preferential localization of SSEA-4 in interfaces between blastomeres of mouse preimplantation embryos

Ban Sato ^{a,c}, Yohko U. Katagiri ^{a,d,*}, Kenji Miyado ^b, Hidenori Akutsu ^b, Yoshitaka Miyagawa ^a, Yasuomi Horiuchi ^a, Hideki Nakajima ^a, Hajime Okita ^{a,d}, Akihiro Umezawa ^b, Jun-ichi Hata ^a, Junichiro Fujimoto ^{c,d,1}, Kiyotaka Toshimori ^e, Nobutaka Kiyokawa ^{a,d}

^a Department of Developmental Biology, National Research Institute for Child Health and Development, 2-10-1 Okura, Setagaya-ku, Tokyo 157-8535, Japan

^b Department of Reproductive Biology, National Research Institute for Child Health and Development, 2-10-1 Okura, Setagaya-ku, Tokyo 157-8535, Japan

^c National Research Institute for Child Health and Development, 2-10-1 Okura, Setagaya-ku, Tokyo 157-8535, Japan

^d Core Research for Evolutional Science and Technology (CREST) of Japan Science and Technology Corporation (JST), Japan

^e Department of Anatomy and Developmental Biology, Graduate School of Medicine, Chiba University, Chiba 260-8670, Japan

Received 11 October 2007

Available online 26 October 2007

Abstract

The monoclonal antibody 6E2 raised against the embryonal carcinoma cell line NCR-G3 had been shown to also react with human germ cells. Thin-layer chromatography (TLC) immunostaining revealed that 6E2 specifically reacts with sialosylglobopentaosylceramide (sialylGb5), which carries an epitope of stage-specific embryonic antigen-4 (SSEA-4), known as an important cell surface marker of embryogenesis. The immunostaining of mouse preimplantation embryos without fixation showed that the binding of 6E2 caused the clustering and consequent accumulation of sialylGb5 at the interface between blastomeres. These results suggest that SSEA-4 actively moves on the cell surface and readily accumulates between blastomeres after binding of 6E2.

© 2007 Elsevier Inc. All rights reserved.

Keywords: SialylGb5; SSEA-4; Embryonic stem cells; Embryonal carcinoma cells; Preimplantation embryo; Immunostaining

Embryonal carcinoma (EC) cells isolated from teratocarcinomas have been shown to possess pluri- or multipotency in both mouse and human systems [1–3]. In mice, certain EC cells as well as embryonic stem (ES) cells have been considered to be developmentally equivalent to the inner cell mass of blastocysts [1]. These EC cells are useful for clarifying the molecular characteristics of early embryonic cells and thus many efforts have been made to establish EC cell lines and monoclonal antibodies (Mabs) that

detect differentiation-related molecules on EC cells. As a consequence, a number of stage-specific markers for embryogenesis have been identified. Notably, it is important that this molecular information is adapted to research on ES cells or mouse preimplantation embryos. Stage-specific embryonic antigen (SSEA) -1, -3, and -4, as well as tumor rejection antigen (TRA) -1-60 and -1-81 [4], have been used as stage-specific markers for embryogenesis, though their functional significance in early development remains unclear. Interestingly, however, most of these antigens are carbohydrates themselves or closely related to the carbohydrates carried on glycosphingolipids (GSLs) and glycoproteins [5].

6E2 is a Mab established by immunizing with NCR-G3 cells, a previously established multipotent human EC cell

* Corresponding author. Address: Department of Developmental Biology, National Research Institute for Child Health and Development, 2-10-1 Okura, Setagaya-ku, Tokyo 157-8535, Japan. Fax: +81 3 3417 2496.

E-mail address: kata@nch.go.jp (Y.U. Katagiri).

¹ Vice General Director.

line capable of differentiating into trophoblastic cell lineages other than somatic cells [3]. It has been revealed that 6E2 reacts with not only human ECs, including NCR-G2 and 3 cells, but also other germ cell tumors, as well as normal human germ cells such as spermatogonia and oocytes [6]. Although a previous study reported that 6E2 immunoprecipitates a cell surface protein having a molecular weight of approximately 80 kDa from 125 I-labeled NCR-G3 cells, the specific antigen recognized by 6E2 still remains unknown. To characterize the antigen specificity of 6E2, we examined the reactivity of the Mab with other cell lines using several distinct methods. In this paper, we present evidence that 6E2 recognizes SSEA-4 carried by sialylGb5. Using 6E2, we determined the localization of SSEA-4 in “living” mouse preimplantation embryos and observed its preferential localization in interface between blastomeres.

Materials and methods

Cells, antibodies, and animals. The human renal carcinoma cell line ACHN was purchased from American Type Culture Collection. The African green monkey kidney cell line Vero was a gift from Dr. T. Takeda of Department of Infectious Diseases Research, National Children's Medical Research Center, Tokyo, Japan. Cells were maintained in Dulbecco's modified Eagle's minimum essential medium (DMEM) (Sigma Chem., St. Louis, MO) supplemented with 10% fetal bovine serum (FBS) (JRH Bioscience, Lenexa, KS). The human EC cell line NCR-G2 [3] was cultured in a 1:1 mixture of DMEM and Ham's F12 medium (DMEM/F12) (Invitrogen Gibco, Carlsbad, CA) supplemented with 10% FBS (JRH Bioscience), non-essential amino acid solution (NEAA) (Invitrogen Gibco), and Insulin-Transferrin-Sodium Selenite media (Invitrogen Gibco). The cynomolgus monkey ES cell line CMK-6 [7] were provided by Dr. Yasushi Kondo of Mitsubishi Tanabe Pharma Corporation. ES cells were grown on mouse embryonic fibroblast feeder cells that were inactivated by gamma-irradiation in DMEM/F12 supplemented with 20% Knockout™ Serum Replacement, 2 mM Glutamax-I, 1% NEAA, 50 units/ml penicillin, 50 µg/ml streptomycin, 0.1 mM 2-mercaptoethanol, 1% sodium pyruvate, and 5 ng/ml bFGF (all from Invitrogen GIBCO). The cultures were performed at 37°C in a 5% CO₂ incubator. The human venous blood from a healthy consenting volunteer was drawn in a heparin-coated syringe. The blood was spun at 3000 rpm for 15 min and human red blood cells (hRBCs) were washed three times in phosphate buffered saline (PBS).

The conjugation of affinity-purified 6E2 (mouse IgG₃, κ) [6] to the fluorescence reagent was performed with an Alexa Fluor® 488 monoclonal antibody labeling kit (Molecular Probes, Eugene, OR.) according to the manufacturer's instructions. The anti-SSEA-4 Mabs used in this study were Raft.2 [8] and MC813-70 (R&D Systems, Inc Minneapolis, MN). Alexa Fluor® 488 goat anti-mouse IgG and Streptavidin Alexa Fluor® 568 were purchased from Molecular probes.

BDF1 mice were purchased from Clea Japan (Tokyo, Japan).

TLC immunostaining of GSLs. TLC immunostaining of GSLs from cultured cells and hRBCs was performed as previously described [9]. Reference GSLs were purchased from Matlayer, Inc. (Pleasant Gap, PA). SialylGb5 was purified from ACHN cells by preparative TLC. Purified GM1 b was kindly provided by Dr. Nakamura of RIKEN, Saitama, Japan [10].

Flow cytometry. Cells were harvested and incubated with a primary antibody (1 µg/ml) for 1 h on ice, followed by treatment with fluorescein isothiocyanate-conjugated goat anti-mouse immunoglobulins (Jackson ImmunoResearch Laboratories, Inc., West Grove, PA) at a dilution of 1:50 and analyzed with an EPICS-XL flow cytometer (Beckman Coulter, Inc. Miami, FL).

Dot blot analysis. Purified sialylGb5 was serially diluted (0.1–60 ng) and vacuum blotted onto a PVDF membrane by using a 96-well format

dot blot apparatus (Bio-Rad Laboratories, Richmond, CA). The membrane was immunostained with the Mab 6E2 or MC813-70 (0.5 µg/ml) according to a previously described procedure [9]. The antibodies that bound to the membranes were visualized with ECL-plus Western Blotting Detection Reagents (GE Healthcare UK Ltd, Buckinghamshire, UK) and scanned with a LAS-1000 luminescent imaging analyzer (Fujifilm, Tokyo, Japan). Scanned images were analyzed using the software Image Gauge with which the LAS-1000 was equipped.

Indirect immunostaining of cynomolgus monkey ES cells. Cells were grown on a glass-bottomed dish (IWAKI) for 3 days and then these cells were fixed for 30 min with 4% paraformaldehyde in PBS and permeabilized with 0.2% Triton X-200 in PBS for 20 min. Subsequently, the cells were washed three times with PBS for 5 min and blocked with 5% normal goat serum in PBS for 30 min. The fixed cells were incubated with anti-SSEA-4 antibodies or isotype-matched mouse IgG at a dilution of 1:300 for 2 h, followed by incubation with Alexa Fluor® 488-conjugated goat anti-mouse IgG at a dilution of 1:300 for 30 min. DAPI was used for counter staining of nuclei.

Immunostaining of mouse preimplantation embryos. Mouse preimplantation embryos were collected from superovulated mice. Seven-week-old BDF1 female mice were induced to superovulate with intraperitoneal injections of pregnant mare's serum gonadotropin (ASKA Pharmaceutical co., Ltd., Tokyo, Japan) (5 IU) and human chorionic gonadotropin (hCG) (ASKA Pharmaceutical co) (5 IU) 48 h apart and mated with individual BDF1 male mice after the hCG injection. The 2-cell, the 8-cell, and the morula stage embryos were flushed out from oviducts at 36, 60, and 72 h after the hCG injection, respectively. Animals were treated according to the institutional animal care and use guidelines of National Research Institute for Child Health and Development.

Embryos immediately after being collected and those prefixed with 2% paraformaldehyde in HEPES buffered saline were incubated in 30 µl drops of M16 medium containing 0.45 µg of Alexa Fluor® 488-conjugated 6E2 for 1 h or biotinylated MC813-70 for 1 h, treated with streptavidin Alexa Fluor® 568 diluted 1:300, and then they were washed three times in 30 µl drops of M16 medium. All staining steps were carried out at 37°C in a CO₂ incubator for fresh embryos and at 4°C for fixed embryos. The stained embryos were placed in drop of a M16 medium on glass-bottomed dishes (IWAKI, Tokyo, Japan), and were observed with a LSM510 Zeiss Confocal laser-scanning microscope (Carl Zeiss, Thornwood, NY) to obtain a field of view of the embryo only with a 40x objective lens.

Results and discussion

6E2 specifically binds to sialylGb5

In order to examine whether the 80 kDa membrane protein is recognized by 6E2, we performed a Western analysis of the cell lysates or their immunoprecipitates with 6E2. Since no significant signal was detected on the blot (data not shown), we examined TLC immunostaining of GSLs extracted from several 6E2-positive cell lines. ACHN cells showed the expression of comparable amounts of Gb3, Gb4, Gb5, and sialylGb5, whereas Vero cells and NCR-G2 cells expressed predominantly Gb3 (Fig. 1A). TLC immunostaining analysis revealed that 6E2 binds to a major slow-migrating GSL extracted from these three cell lines. The slow-migrating GSL was identified as sialylGb5, defined by the Mab Raft.2. We observed that 6E2 bound to sialylGb5 (LKE-antigen) of hRBCs [13] (Fig. 1B). Finally, we examined the reactivity of 6E2 with purified GSLs and found that the Mab reacts with purified sialylGb5, but not purified GM1 b (Fig. 1C). These results indicate that 6E2 specifically binds to sialylGb5 and thus is an anti-SSEA-4

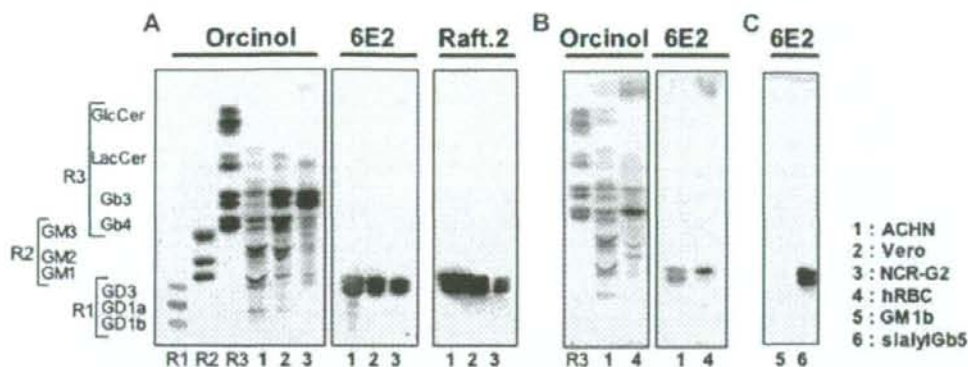


Fig. 1. TLC immunostaining of GSLs prepared from cultured cells and hRBCs. GSLs extracted from cultured cells and hRBCs or purified GSLs were separated by TLC in a solvent system of chloroform/methanol/water containing 0.2% CaCl_2 (5:4:1, v/v/v). Plates were chemically stained with orcinol-sulfuric acid or were immunostained with 6E2 and Raft.2. Lane 1, ACHN; Lane 2, Vero; Lane 3, NCR-G2; Lane 4, hRBCs; Lane 5, GM1b; Lane 6, sialylGb5. Reference markers used were disialosyl gangliosides of GD3, GD1a, and GD1b (R1), monosialosyl gangliosides of GM3, GM2, and GM1 (R2), and neutral GSLs of GlcCer, LacCer, Gb3, and Gb4 (R3). The nomenclature for GSLs follows the recommendations [11] of the IUB, and the ganglioside nomenclature of Svennerholm [12] was used.

Mab. The 80 kDa protein might be associated with sialylGb5 in NCR-G3 cells and thus co-immunoprecipitated by 6E2.

Comparison of reactivity to sialyl Gb5 between 6E2 and MC813-70

MC813-70 established by immunizing with human EC cell lines has been most widely used as an anti-SSEA-4 anti-

body (mouse IgG₃, κ) [14]. Therefore we compared the reactivities of the Mabs 6E2 and MC813-70 by flow cytometry and dot-blot immunostaining. The fluorescence intensity obtained with 6E2 was stronger than that with MC813-70 in each cell line and hRBCs (Fig. 2A). A recent flow cytometric study showed that MC813-70 strongly stains hRBCs, but other anti-sialylGb5 Mabs do not [15]. However, our data indicate that 6E2 is more reactive than MC813-70. Next we compared the reactivity of the two

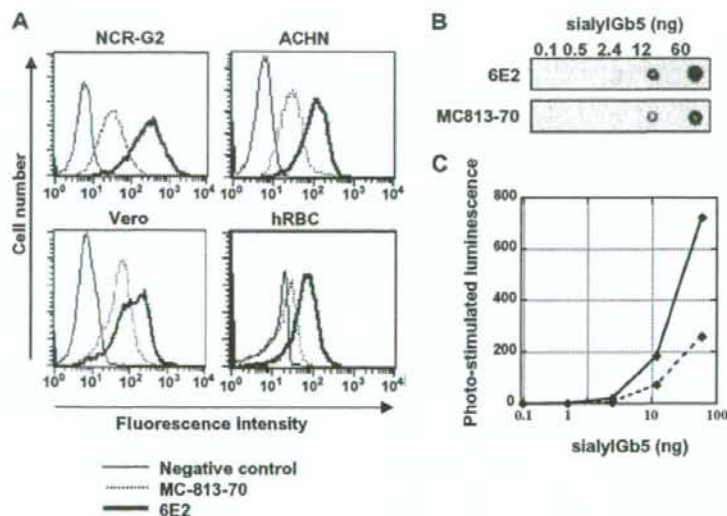


Fig. 2. Reactivity of 6E2 and MC813-70 with sialylGb5. (A) Flow cytometric analysis of SSEA-4-positive cells with 6E2. NCR-G2 cells, ACHN cells, Vero cells, and hRBCs were stained with 6E2 (bold line) or MC813-70 (dotted line) and with a FITC-conjugated secondary antibody and analyzed by flow cytometry. (B) An image of the dot-blot immunostaining of sialylGb5 obtained with a LAS-1000 luminescent imaging analyzer. (C) Measurement of antibodies bound (6E2: solid line, MC813-70: broken line).

Mabs with that of sialylGb5 by dot-blot immunostaining. Serially diluted sialylGb5 was dot-blotted onto a PVDF membrane, and the membrane was immunostained with the two Mabs. Both 6E2 and MC813-70 bound to more than 12 ng of sialylGb5, but the signals induced by 6E2 were stronger than those induced by MC813-70 (Fig. 2B,C). Thus, in addition to the flow cytometric analysis, the reactivity of 6E2 with sialylGb5 was stronger than that of MC813-70 by dot-blot immunostaining.

SSEA-4 Immunostaining of cynomolgus monkey ES cells

To confirm whether Mab 6E2 reacts with SSEA-4 on monkey ES cells, we performed an indirect immunofluorescence staining of cynomolgus monkey ES cells with Mab 6E2 and MC813-70. Mab 6E2 reacted with monkey ES cells (Fig. 3A) as well as MC-813-70 did (Fig. 3B). No difference in staining patterns of SSEA-4 between the two Mabs was observed. Mab 6E2 certainly stained SSEA-4 on monkey ES cells.

SSEA-4 immunostaining of "living" mouse preimplantation embryos without fixation

During early embryogenesis in mice, SSEA-4 had been reported to be expressed in fertilized eggs with levels gradually increasing to the morula stage and then decreasing [5]. Thus we examined the expression and distribution of SSEA-4 in preimplantation mouse embryos by immunostaining with both 6E2 and MC813-70. Both Mabs evenly stained the whole surface membranes of fixed mouse embryos, and no difference in staining pattern between the two was observed (data not shown). In order to perform a time-course of SSEA-4 distribution in a viable state, we performed immunostaining of preimplantation embryos without fixation.

3D-images of the 6E2 staining pattern obtained by confocal laser scanning microscopic observation clearly showed the localization of SSEA-4 on mouse preimplantation embryos. Two-cell embryos showed patches of SSEA-4 over the whole surface membrane with some accumulation at the interface between blastomeres (Fig. 4A). In 8-cell embryos, the amount accumulated at interfaces was further increased, as if planer membranes

separate each blastomere, and some large patches were internalized but others were left on the surface membranes (Fig. 4B). The amount of SSEA-4 concentrated at the interfaces in morula was not as significant as in 8-cell embryos but still clearly observed and some patches were internalized (Fig. 4C).

2D-images of embryos stained with 6E2 showed a marked accumulation of SSEA-4 at the interfaces between blastomeres (Fig. 4D–F). These results suggest that sialylGb5 actively moves during development and tends to accumulate where blastomeres come into contact with each other.

Interestingly, however, the staining pattern of SSEA-4 using MC813-70 was different from that using 6E2. MC813-70 evenly stained the surface and the interface between blastomeres of 2-cell embryos with patches (Fig. 4G), and the amount of SSEA-4 at interfaces was not significant (Fig. 4J). In 8-cell embryos, there were patches of SSEA-4 in the central area of the outer surface of each blastomere (Fig. 4H, indicated by arrows), but the 2D-image showed that clustering also occurred at surfaces facing blastocoels (Fig. 4K, indicated by arrowheads). In morula embryos, SSEA-4 was distributed on the surface in patches and was enriched at the boundaries between blastomeres on the outer surface (Fig. 4I,L).

It remains unclear why the pattern of staining of mouse preimplantation embryos differs between 6E2 and MC813-70. The composition of fatty acids in GSLs influences the binding of antibodies [16,17] or bacterial toxins [18]. SialylGb5 recognized by the two Mabs might differ in composition of fatty acids, resulting in different immunostaining patterns. It was reported that the clustering of sialylGb5 by a Mab induces the activation of sialylGb5-associated kinases in raft microdomains of human mammary carcinoma cells, leading to downstream signaling [19,20]. The clustering of sialylGb5 by 6E2 on preimplantation mouse embryos may also induce the activation of some kinases, followed by downstream signaling. Recently, Comisky et al. suggested that lipid rafts and their associated molecules are spatiotemporally positioned to play a critical role in preimplantation developmental events [21]. The patches or clusters of sialylGb5 shown in our study suggest the presence of lipid rafts containing sialylGb5 on mouse embryos.



Fig. 3. Indirect immunostaining of cynomolgus monkey ES cell line CMK-6 with 6E2 and MC813-70. The CMK-6 cells were stained with 6E2 (A), MC813-70 (B), or isotype-matched mouse IgG (C), and visualized with secondary antibodies (green), followed by counterstaining of nuclei with DAPI (blue). Scale bars = 200 μ m.

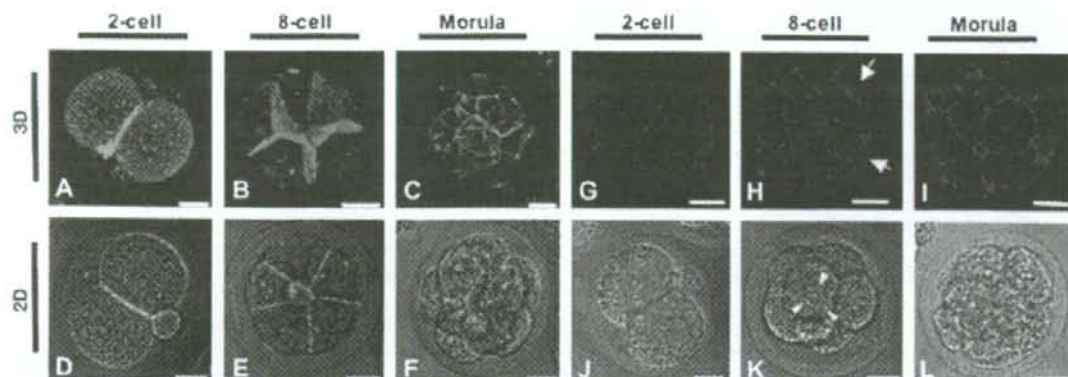


Fig. 4. Immunostaining of SSEA-4 on mouse preimplantation embryos with 6E2 and MC813-70. The embryos at the 2-cell (A, D, G, J), the 8-cell (B, E, H, K), and the morula (C, F, I, L) stages were stained with 6E2 (green) or MC813-70 (red). The panels designated 3D (A, B, C, G, H, I) are three-dimensional images reconstructed by stacking optical slice images using LSM software and the panels designated 2D (D, E, F, J, K, L) are an overlay of a fluorescent image and a differential interference contrast micrograph. Scale bars = 20 μ m.

6E2 has high affinity for sialylGb5 and can be effectively conjugated with fluorescence reagents, leading to excellent staining of SSEA-4 in the surface membrane of "living" mouse preimplantation embryos. 6E2 should be of use for research into lipid rafts in early development and of great advantage for the characterization of ES cells and EC cells.

Acknowledgments

We thank S. Yamauchi for her excellent secretarial work. This work was supported in part by grants from CREST of JST and the 3rd. term comprehensive 10-year-strategy for cancer control, Research on Children and Families, Research on Human Genome Tailor made and Research on Publicly Essential Drugs and Medical Devices, Health and Labour Sciences Research Grants from the Ministry of Health, Labour and Welfare of Japan and a grant from The Japan Leukemia Research Field.

References

- [1] B. Mintz, K. Illmensee, Normal genetically mosaic mice produced from malignant teratocarcinoma cells, *Proc. Natl. Acad. Sci. USA* 72 (1975) 3585–3589.
- [2] P.W. Andrews, I. Damjanov, D. Simon, G.S. Banting, C. Carlin, N.C. Dracopoli, J. Fogh, Pluripotent embryonal carcinoma clones derived from the human teratocarcinoma cell line Tera-2. Differentiation *in vivo* and *in vitro*, *Lab Invest.* 50 (1984) 147–162.
- [3] J.F. Jun-ichi Hata, Eizaburo Ishii, Akihiro Umezawa, Yasuo Kokai, Yoshie Matsubayashi, Hiroshi Abe, Satoru Kusakari, Haruto Kikuchi, Taketo Yamada, Tatsuya Maruyama, Differentiation of human germ cell tumor cells *in vivo* and *in vitro*, *Acta Histochem. Cytochem.* 25 (1992) 563–576.
- [4] J.S. Draper, C. Pigott, J.A. Thomson, P.W. Andrews, Surface antigens of human embryonic stem cells: changes upon differentiation in culture, *J. Anat.* 200 (2002) 249–258.
- [5] T. Muramatsu, H. Muramatsu, Carbohydrate antigens expressed on stem cells and early embryonic cells, *Glycoconj. J.* 21 (2004) 41–45.
- [6] T. Nakano, A. Umezawa, H. Abe, N. Suzuki, T. Yamada, S. Nozawa, J. Hata, A monoclonal antibody that specifically reacts with human embryonal carcinomas, spermatogonia and oocytes is able to induce human EC cell death, *Differentiation* 58 (1995) 233–240.
- [7] M. Yamamoto, N. Tase, T. Okuno, Y. Kondo, S. Akiba, N. Shimozawa, K. Terao, Monitoring of gene expression in differentiation of embryoid bodies from cynomolgus monkey embryonic stem cells in the presence of bisphenol A, *J. Toxicol. Sci.* 32 (2007) 301–310.
- [8] Y.U. Katagiri, K. Ohmi, C. Katagiri, T. Sekino, H. Nakajima, T. Ebata, N. Kiyokawa, J. Fujimoto, Prominent immunogenicity of monosialosyl galactosylgloboside, carrying a stage-specific embryonic antigen-4 (SSEA-4) epitope in the ACHN human renal tubular cell line—a simple method for producing monoclonal antibodies against detergent-insoluble microdomains/raft, *Glycoconj. J.* 18 (2001) 347–353.
- [9] Y.U. Katagiri, N. Kiyokawa, K. Nakamura, H. Takenouchi, T. Taguchi, H. Okita, A. Umezawa, J. Fujimoto, Laminin binding protein, 34/67 laminin receptor, carries stage-specific embryonic antigen-4 epitope defined by monoclonal antibody Raft.2, *Biochem. Biophys. Res. Commun.* 332 (2005) 1004–1011.
- [10] K. Nakamura, Y. Hashimoto, M. Suzuki, A. Suzuki, T. Yamakawa, Characterization of GM1b in mouse spleen, *J. Biochem. (Tokyo)* 96 (1984) 949–957.
- [11] The nomenclature of lipids (recommendations 1976). IUPAC-IUB Commission on Biochemical Nomenclature, *J. Lipid. Res.* 19 (1978) 114–128.
- [12] L. Svennerholm, Designation and schematic structure of gangliosides and allied glycosphingolipids, *Prog. Brain Res.* 101 (1994) XI–XIV.
- [13] L.L. Cooling, K. Kelly, Inverse expression of P(k) and Luke blood group antigens on human RBCs, *Transfusion* 41 (2001) 898–907.
- [14] L.H. Shevinsky, B.B. Knowles, I. Damjanov, D. Solter, Monoclonal antibody to murine embryos defines a stage-specific embryonic antigen expressed on mouse embryos and human teratocarcinoma cells, *Cell* 30 (1982) 697–705.
- [15] L. Cooling, D. Hwang, Monoclonal antibody B2, a marker of neuroendocrine sympathoadrenal precursors, recognizes the Luke (LKE) antigen, *Transfusion* 45 (2005) 709–716.
- [16] K. Iwabuchi, I. Nagaoka, Lactosylceramide-enriched glycosphingolipid signaling domain mediates superoxide generation from human neutrophils, *Blood* 100 (2002) 1454–1464.
- [17] K. Iwabuchi, Y. Zhang, K. Handa, D.A. Withers, P. Sinay, S. Hakomori, Reconstitution of membranes simulating "glycosignaling

- domain" and their susceptibility to lyso-GM3, *J. Biol. Chem.* 275 (2000) 15174–15181.
- [18] A. Kiarash, B. Boyd, C.A. Lingwood, Glycosphingolipid receptor function is modified by fatty acid content. Verotoxin 1 and verotoxin 2c preferentially recognize different globotriaosyl ceramide fatty acid homologues, *J. Biol. Chem.* 269 (1994) 11138–11146.
- [19] W.F. Steelant, Y. Kawakami, A. Ito, K. Handa, E.A. Bruyneel, M. Mareel, S. Hakomori, Monosialyl-Gb5 organized with cSrc and FAK in GEM of human breast carcinoma MCF-7 cells defines their invasive properties, *FEBS Lett.* 531 (2002) 93–98.
- [20] S. Van Slambrouck, W.F. Steelant, Clustering of monosialyl-Gb5 initiates downstream signalling events leading to invasion of MCF-7 breast cancer cells, *Biochem. J.* 401 (2007) 689–699.
- [21] M. Comiskey, C.M. Warner, Spatio-temporal localization of membrane lipid rafts in mouse oocytes and cleaving preimplantation embryos, *Dev. Biol.* 303 (2007) 727–739.

Metformin Suppresses Interleukin (IL)-1 β -Induced IL-8 Production, Aromatase Activation, and Proliferation of Endometriotic Stromal Cells

Yuri Takemura, Yutaka Osuga, Osamu Yoshino, Akiko Hasegawa, Tetsuya Hirata, Yasushi Hirota, Emi Nose, Chieko Morimoto, Miyuki Harada, Kaori Koga, Toshiki Tajima, Tetsu Yano, and Yuji Taketani

Department of Obstetrics and Gynecology, Faculty of Medicine, University of Tokyo, Tokyo 113-8655, Japan

Context: Metformin, a widely used treatment for diabetes that improves insulin sensitivity, also has both antiinflammatory properties and a modulatory effect on ovarian steroid production, two actions that have been suggested to be efficacious in therapy for endometriosis.

Objective: To determine whether metformin may be effective for the treatment of endometriosis, we evaluated the effects of this agent on inflammatory response, estradiol production, and proliferation of endometriotic stromal cells (ESCs).

Design: ESCs derived from ovarian endometriomas were cultured with various concentrations of metformin.

Main Outcome Measures: IL-8 production, mRNA expression and aromatase activity, and 5-bromo-2'-deoxyuridine incorporation in ESCs were measured.

Results: Metformin dose-dependently suppressed IL-1 β -induced IL-8 production, cAMP-induced mRNA expression and aromatase activity, and 5-bromo-2'-deoxyuridine incorporation in ESCs.

Conclusion: These results suggest that further investigation into the unique therapeutic potential of metformin as an antiendometriotic drug is warranted. (*J Clin Endocrinol Metab* 92: 3213-3218, 2007)

METFORMIN IS A widely used antidiabetic agent that improves insulin sensitivity (1). In reproductive medicine, the drug has been successfully used for the treatment of polycystic ovary syndrome, an etiology of which is suggested to be insulin resistance (2). Metformin may also reduce obesity-associated inflammatory status and other inflammatory responses (3-5), and has reduced serum C-reactive protein levels in women with polycystic ovary syndrome (6). In addition, it has direct effects on steroidogenesis in ovarian granulosa cells and thecal cells (7, 8).

Endometriosis is an estrogen-dependent enigmatic disease that deteriorates the health of women of reproductive age (9, 10). A large body of evidence suggests that the peritoneal inflammatory environment stimulates progress of the disease (10-14), and we and others have shown that antiinflammatory drugs have therapeutic potential for the disease (15-18). Metformin, in addition to antiinflammatory properties, has a possible modulatory effect on local steroid production, suggesting it may be active against endometriosis.

Endometriosis is characterized by inflammation, estrogen dependency, and proliferation of endometriotic cells. Here, we have evaluated the effects of metformin on markers of these pathophysiological processes in endometriotic cells as

a first step toward evaluating its therapeutic application in this condition.

Subjects and Methods

Reagents and materials

Type I collagenase and antibiotics (penicillin, streptomycin, and amphotericin B) were purchased from Sigma-Aldrich (St. Louis, MO). DMEM/Ham's F12 (F-12) medium, 0.25% trypsin-EDTA, and 0.4% trypan blue stain were from Life Technologies, Inc. (Grand Island, NY). L, 1-Dimethylbiguanide hydrochloride (metformin), 8-bromo-cAMP, and 4-androstene-3, 17-dione (androstenedione) were obtained from Sigma-Aldrich. Recombinant IL-1 β was purchased from Genzyme/Techne (Minneapolis, MN). Charcoal-stripped fetal bovine serum (FBS) was from HyClone (Logan, UT). Deoxyribonuclease I was from Invitrogen (Carlsbad, CA).

Collection of samples

Endometriotic tissues were obtained from women undergoing laparoscopy or laparotomy for ovarian endometriomas. In total, 38 women aged 24-45 yr were recruited to the present study. All women had regular menstrual cycles, and none had received hormonal treatment for at least 6 months before surgery. Symptoms of the women were pain (n = 26), infertility (n = 2), both pain and infertility (n = 6), and neither (n = 4). Menstrual phases at operation were proliferative in 18 patients and secretory in 20. Stages of endometriosis were III (n = 17) and IV (n = 21). The endometriotic tissue samples were collected from the cyst walls of ovarian endometriomas under sterile conditions for primary cell cultures.

The experimental procedures were approved by the institutional review board of the University of Tokyo, and signed informed consent for use of the sample was obtained from each woman.

Isolation and culture of human endometriotic stromal cells (ESCs)

Human ESCs were isolated and cultured as described previously (12, 19, 20). Fresh endometriotic specimens collected in sterile medium were

First Published Online May 15, 2007

Abbreviations: AMPK, AMP-activated protein kinase; BrdU, 5-bromo-2'-deoxyuridine; ESC, endometriotic stromal cell; FBS, fetal bovine serum; GAPDH, glyceraldehyde-3-phosphate dehydrogenase; LDH, lactate dehydrogenase; PPAR, peroxisome proliferator-activated receptor.

JCEM is published monthly by The Endocrine Society (<http://www.endo-society.org>), the foremost professional society serving the endocrine community.

rinsed to remove blood cells. The tissues were minced into small pieces and incubated in DMEM/F-12, containing 25 mg/ml type I collagenase and 15 U/ml deoxyribonuclease I, for 2–3 h at 37°C, and separated using serial filtration. Debris was removed with a 100- μ m nylon cell strainer (Becton Dickinson and Co., Franklin Lakes, NJ), and dispersed epithelial glands were eliminated by filtration through a 70- μ m nylon cell strainer (Becton Dickinson and Co.). ESCs in the filtrate were collected by centrifugation and resuspended in phenol red-free DMEM/F-12 containing 10% charcoal-stripped FBS, 100 U/ml penicillin, 100 μ g/ml streptomycin, and 250 ng/ml amphotericin B. The ESCs were seeded in a 100-mm culture plate and kept at 37°C in a humidified 5% CO₂/95% air atmosphere. At the first passage, the cells were plated into 6-, 24-, 48-, or 96-well culture plates (Becton Dickinson and Co.) at a density of 2×10^5 cells/ml in medium supplemented with 10% FBS.

The purity of the stromal cell preparations was more than 95%, as judged by positive cellular staining for vimentin and negative cellular staining for cytokeratin, CD45, CD68, and von Willebrand factor.

Measurement of IL-8

When the ESCs were approaching confluence, media were removed and replaced with fresh media and antibiotics, and the cells were cultured in serum-free media for an additional 12 h. Subsequently, the cells were incubated with or without metformin (10, 100, and 1000 μ M) in serum-free media for 24 h and then stimulated with 5 ng/ml IL-1 β in serum-free media for 24 h, according to our previous study (14, 20, 21). Metformin was dissolved in distilled water and then diluted 1:1000 in the medium. The doses of metformin used in the present study are similar to those used in other studies examining *in vitro* effects of metformin (4, 22). In addition, the peak plasma concentration of the drug at a standard dosage is approximately 10–20 μ M (23, 24). Because local application of an antiendometriotic drug is desirable (25), we also tested metformin at relatively high concentrations. Concentrations of IL-8 in conditioned culture media were measured using a specific ELISA kit (Quantikine; R&D Systems, Minneapolis, MN) according to the manufacturer's protocol. Data were standardized by total protein of cell lysates.

RNA extraction, reverse transcription, and real-time quantitative PCR of aromatase

When the ESCs were approaching confluence, media were replaced with fresh media and antibiotics, and the cells were cultured in serum-free media for an additional 12 h. Subsequently, the cells were incubated with or without metformin (10, 100, and 1000 μ M) for 24 h, and then stimulated with 1 mM cAMP for 24 h. Total RNA was extracted from the ESCs, using an RNeasy minikit (QIAGEN, Hilden, Germany). The quality of the total RNA thus obtained was confirmed by determining appropriate sharp 28S and 18S rRNA bands by agarose gel electrophoresis. One microgram of total RNA was reverse transcribed in a 20- μ l volume using ReverTra Ace- α (TOYOBO Co., Ltd., Osaka, Japan).

Aromatase mRNA expression was assessed by real-time quantitative PCR using a LightCycler according to the manufacturer's instructions (Roche Diagnostic GmbH, Mannheim, Germany). Aromatase primers (sense, 5'-CAGAGGCCAAGAGTTGAGG-3'; antisense, 5'-ACAC-TAGCAGGTGGGTTTGG-3') were chosen to amplify a 243-bp fragment. Human glyceraldehyde-3-phosphate dehydrogenase (GAPDH) primers (TOYOBO Co., Ltd.) were used to measure GAPDH mRNA levels so that expression of aromatase mRNA could be normalized to RNA loading for each sample. PCR conditions were as follows: for aromatase, 30 cycles at 95°C for 15 sec, 64°C for 8 sec, and 72°C for 10 sec; and for GAPDH, 25 cycles at 95°C for 15 sec, 64°C for 10 sec, and 72°C for 18 sec. All these PCR conditions were followed by melting curve analysis.

Each PCR product was purified with a QIAEX II gel extraction kit (QIAGEN), and their identities were confirmed using an ABI PRISM 310 genetic analyzer (Applied Biosystems, Foster City, CA).

Aromatase assay

The effect of metformin on aromatase activity was evaluated by measuring estrone levels in conditioned media of ESCs cultured with androstenedione. ESCs were seeded into 24-well plates at a density of 1×10^5 cells per well in 500 μ l of the culture medium. After the ESCs

were approaching confluence, the medium was replaced with fresh medium containing 2.5% FBS. The cells were incubated with or without metformin (10, 100, and 1000 μ M) for 24 h and then stimulated with 1 mM cAMP for 24 h. After the treatments, 5 nM androstenedione was added to each well, and ESCs were incubated for another 24 h. The conditioned media were collected, centrifuged, and stored at -80°C for measurement of estrone levels.

Measurement of estrone

Concentrations of estrone in conditioned culture media were measured using a specific Estrone EIA kit (Yanaihara Institute Inc., Shizuoka, Japan) according to the manufacturer's protocol (26). Data were standardized by total protein of cell lysates.

5-Bromo-2'-deoxyuridine (BrdU) proliferation assay

The effect of metformin on the proliferation of ESCs was examined by measuring incorporation of BrdU into DNA. The assay was performed using a Biotrak cell proliferation ELISA system (Amersham Biosciences, Little Chalfont, UK), as previously described (12, 19, 20). Briefly, ESCs were seeded into 96-well plates at a density of 5×10^3 cells per well in 100 μ l culture medium. After 24 h, the medium was replaced with fresh medium containing 2.5% FBS. After 24 or 48 h of treatment with or without metformin (10, 100, and 1000 μ M), 100- μ l BrdU solutions were added and incubated at 37°C for an additional 2 h. The culture medium was then removed, and the cells were fixed, and the DNA was denatured by the addition of fixative at 200 μ l/well. The peroxidase-labeled anti-BrdU bound to the BrdU incorporated in newly synthesized, cellular DNA. The immune complexes were detected by the subsequent substrate reaction, and the resultant color was read at 450 nm in a DigiScan microplate reader (ASYH Hithec GmbH, Eugendorf, Austria).

Measurement of lactate dehydrogenase (LDH) release and trypan blue exclusion test

LDH release measurement and trypan blue exclusion test were conducted to examine the effect of metformin treatment on cell viability. After ESCs were treated with or without metformin (10, 100, and 1000 μ M) for 24 h, conditioned media were collected, and the cells were dissociated with 0.25% trypsin-EDTA and collected by centrifugation at 200 g for 5 min. The release of LDH into conditioned culture media was measured using a specific Cytotoxicity Detection kit (Roche Diagnostic GmbH) according to the manufacturer's protocol. Assay medium and 2% triton X-100 solution were used for low control and high control, respectively. The ESCs were resuspended in 0.2% trypan blue solution. The number of total or trypan blue stained ESCs was counted using a microscope. Trypan blue-stained ESCs were considered dead.

Statistical analysis

Data were evaluated using ANOVA with *post hoc* analysis for multiple comparisons. *P* values < 0.05 were accepted as significant.

Results

Effects of metformin on IL-1 β -induced IL-8 production in ESCs

IL-8 is a proinflammatory cytokine that has been implicated in the pathogenesis of the disease (11, 12, 14, 19–21, 27). We performed dose-response experiments to determine the effect of metformin on the production of IL-8 in ESCs. The concentrations of IL-8 in all samples were above the lower limit of the assay. Preincubation with metformin significantly decreased IL-1 β -induced IL-8 production in ESCs in a dose-dependent manner compared with controls. The maximal effect was observed at 1000 μ M, but significant decreases were seen at 10 μ M (Fig. 1 and Table 1).

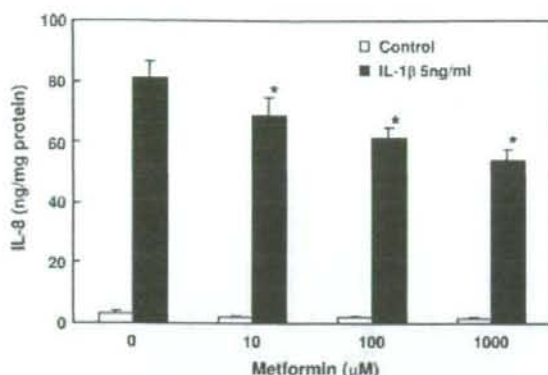


FIG. 1. Effects of metformin on IL-1 β -induced IL-8 production in ESCs. ESCs were incubated with or without metformin (10, 100, and 1000 μ M) for 24 h, and then stimulated with (closed bars) or without (open bars) IL-1 β (5 ng/ml) for 24 h. At the end of the incubation period, conditioned media were collected and assayed for concentrations of IL-8 by ELISA. Values are the mean \pm SEM of quadruplicate cultures. The results are representative of four separate experiments using samples from different women. *, $P < 0.05$ vs. IL-1 β without metformin.

Effects of metformin on cAMP-induced mRNA expression and activity of aromatase in ESCs

Because endometriosis is estrogen dependent, we evaluated the effect of metformin on the expression of aromatase, a critical enzyme for the local production of estrogens that drive the development of the disease (28). We conducted dose-response experiments to determine the effect of metformin on cAMP-induced aromatase mRNA expression in ESCs (Fig. 2A). Metformin decreased cAMP-induced aromatase mRNA levels in ESCs in a dose-dependent manner. The maximum decrease was observed at 1000 μ M, but significant decreases were seen at 100 μ M.

To measure aromatase activity, ESCs were preincubated with metformin for 24 h and then stimulated with cAMP for 24 h. After incubation with 5 nM androstenedione for another 24 h, concentrations of estrone were measured. The concentrations of estrone in all conditioned culture media were above the lower limits of the assay. As depicted in Fig. 2B and Table 1, metformin decreased cAMP-induced aromatase activity in ESCs in a dose-dependent manner, with the maximal effect being observed at 1000 μ M, and significant decreases seen at 10 μ M.

Effects of metformin on BrdU incorporation in ESCs

Dose-response experiments were conducted to determine the effect of metformin on DNA synthesis, as a marker of cell

proliferation, in ESCs. Metformin at concentrations between 10 and 1000 μ M dose dependently inhibited BrdU incorporation into DNA in ESCs at 24 and 48 h of the treatment, the maximal effect being observed at 1000 μ M (Fig. 3 and Table 1).

Effects of metformin on cell viability of ESCs

Metformin did not increase LDH release from ESCs, nor did it increase the number of trypan blue-stained ESCs (Table 2).

Discussion

In the present study, we have demonstrated that metformin suppressed the production of IL-1 β -induced IL-8, the activation of aromatase, and the proliferation of ESCs. These effects of metformin would all be expected to limit the development of endometriosis.

IL-1 β -induced secretion of IL-8 from endometriotic cells has been proposed to be a driver of endometriosis progression (29, 30). IL-8 levels are increased in the peritoneal fluid of women with endometriosis (31, 32). Interestingly, metformin has suppressed IL-8 release from human adipose tissue *in vitro* (33), and a recent report demonstrated that metformin inhibited IL-1 β -induced release of IL-6 and IL-8 in human vascular wall cells (4). Although we show here that metformin can inhibit IL-1 β -induced secretion of IL-8 from ESCs, at the same doses, metformin did not inhibit secretion of IL-8 from eutopic endometrial stromal cells (data not shown). Thus, metformin seems to exert its antiinflammatory role by reducing proinflammatory cytokine secretion in specific cell types.

Because endometriosis is an estrogen-dependent disease, local production of estrogen in endometriotic tissues is suggested to be important for the growth of the lesion. Numerous reports demonstrate abundant aromatase expression and elevated local estrogen production in endometriotic tissues (28), suggesting that aromatase is responsible for the local production of estrogen. Cases of endometriosis have also been successfully treated with aromatase inhibitors (34–38). A fascinating proposed mechanism is that increased prostaglandin estradiol stimulates aromatase activity via cAMP and increases estrogen production in endometriotic lesions (28). In the present study, cAMP-stimulated aromatase activity was suppressed with metformin in ESCs. Thus, metformin could be expected to suppress estrogen levels in endometriotic tissues. Interestingly, metformin has inhibited FSH and insulin-stimulated progesterone and estradiol production in granulosa cells (8). Together, metformin may inhibit endometriosis through suppression of both ovarian and local production of estrogens.

We also show that metformin inhibited BrdU uptake of ESCs. An antiproliferative effect of metformin has also been

TABLE 1. Combined data of responses of ESCs obtained from different patients

Metformin (μ M)	0	10	100	1000
IL-8 (induced by IL-1 and β)	100	87.2 \pm 2.8	80.6 \pm 4.2	71.6 \pm 2.9
Estrone (induced by cAMP)	100	86.1 \pm 5.0	79.2 \pm 2.3	74.8 \pm 4.1
BrdU (24 h)	100	92.9 \pm 1.7	88.9 \pm 2.1	79.4 \pm 4.4
BrdU (48 h)	100	87.0 \pm 3.4	70.7 \pm 5.8	58.9 \pm 5.7

Mean \pm SEM of the data using samples from four different individuals are shown, standardizing values without metformin as 100% in each individual.

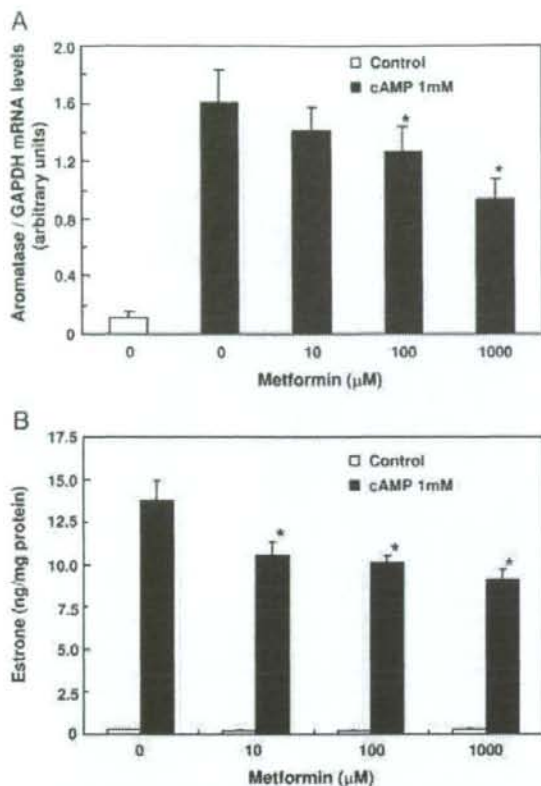


FIG. 2. Effects of metformin on mRNA expression (A) and activity (B) of aromatase induced by cAMP in ESCs. ESCs were incubated with or without metformin (10, 100, and 1000 μM) for 24 h, and then stimulated with (closed bars) or without (open bars) cAMP (1 mM) for 24 h. A, At the end of the incubation period, the total RNA isolated from the ESCs was reverse transcribed and amplified by real-time PCR using primers for aromatase. The data were calculated by subtracting the signal threshold cycles of the internal standard (GAPDH) from aromatase. Values are the mean \pm SEM of six independent experiments. *, $P < 0.05$ vs. cAMP without metformin. B, At the end of the incubation period, androstenedione was added, and cells were incubated for a further 24 h, and conditioned media were collected and assayed for aromatase activity by Estrone EIA kit. Values represent the mean \pm SEM of quadruplicate cultures. The results are representative of four separate experiments using samples from different women. *, $P < 0.03$ vs. cAMP without metformin.

demonstrated in leptin-stimulated vascular smooth muscle cells (39). Combined with the antiinflammatory and antiestrogenic effect of metformin, the direct antiproliferative effect on ESCs supports its therapeutic potential for endometriosis. Consistent with this, one case report described regression of atypical endometrial hyperplasia that was resistant to progestin therapy after metformin treatment (40).

What is an intracellular mechanism that underlies these diverse effects of metformin in ESCs? AMP-activated protein kinase (AMPK) is a known target of metformin action in various cells (22, 41). It is increasingly being shown to have pleiotropic actions in the regulation of the endocrine system.

However, to date, the role of AMPK in endometriosis is unknown. Adiponectin is also an activator of AMPK. We have recently shown that adiponectin stimulated AMPK and inhibited inflammatory cytokine production in endometrial cells (21). In addition, we reported that serum and peritoneal fluid adiponectin levels were decreased in women with endometriosis (42, 43). Together, these suggest that AMPK may be involved in the antiinflammatory effects of metformin demonstrated in ESCs in the present study.

Recently, peroxisome proliferator-activated receptor (PPAR)- γ agonists, ciglitazone (44), and rosiglitazone (45) have regressed endometriotic lesion in a rat endometriosis model. Interestingly, like metformin, these PPAR- γ agonists are also widely used antidiabetic drugs. Similar to metformin, PPAR- γ agonists exert antiinflammatory (46) and antiproliferative effects (47), which are likely to mediate their antiendometriotic properties.

It has been argued that ovarian endometriosis is a different

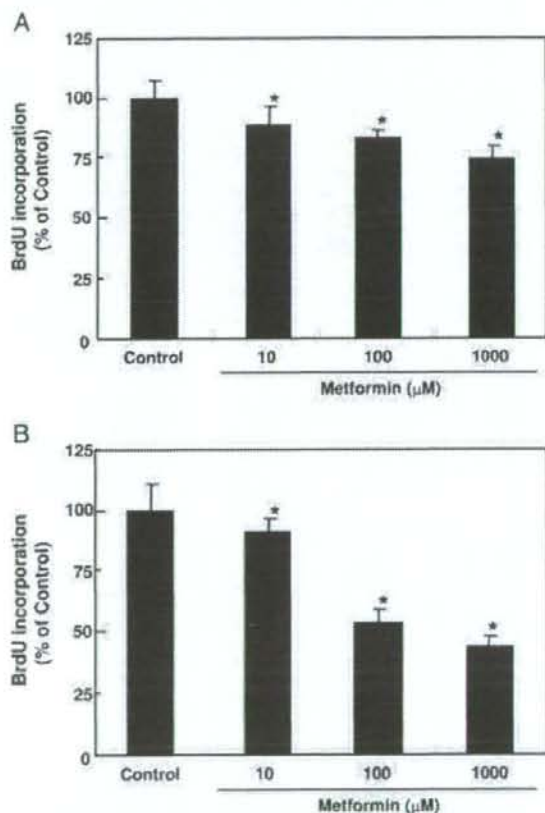


FIG. 3. Effects of metformin on BrdU incorporation in ESCs. The effect of metformin on the proliferation of ESCs was examined by measuring BrdU into DNA by using a cell proliferation ELISA system. ESCs were treated with or without metformin (10, 100, and 1000 μM) for 24 h (A) or 48 h (B). Values are the mean \pm SEM of sextuplicate cultures. The results are representative of four separate experiments using samples from different women. *, $P < 0.01$ vs. control.

TABLE 2. Effects of metformin on LDH release from ESCs and trypan blue staining of ESCs

Metformin (μ M)	0	10	100	1000
LDH	8.6 \pm 1.0	8.3 \pm 1.0	7.8 \pm 1.0	7.1 \pm 0.9
Trypan blue	7.5 \pm 1.3	7.5 \pm 1.4	7.4 \pm 1.8	7.4 \pm 1.2

Mean \pm SEM of the data from four (LDH) and two (trypan blue) independent experiments using ESCs from different individuals is shown. Values are shown as percentage (%) of high control (LDH) and total cells (trypan blue).

entity from peritoneal endometriosis (48), as exemplified by a recent study that showed different patterns of gene expression between ovarian and nonovarian endometriosis (49). Due to technical limitations, we only used endometriotic cells from ovarian endometrioma, and it remains possible that nonovarian endometriotic cells may show different responses to metformin from the present results.

In summary, we have shown that metformin can inhibit IL-1 β -induced IL-8 production, aromatase activation, and proliferation of ESCs. These findings suggest a unique therapeutic potential for metformin as an antiendometriotic drug.

Acknowledgments

Received November 13, 2006. Accepted May 7, 2007.

Address all correspondence and requests for reprints to: Yutaka Osuga, M.D., Department of Obstetrics and Gynecology, Faculty of Medicine, University of Tokyo, 7-3-1, Hongo, Bunkyo-ku, Tokyo 113-8655, Japan. E-mail: yutakaos-tyk@umin.ac.jp.

This work was partially supported by Grants-in-Aid for Scientific Research from the Ministry of Education, Culture, Sports, Science and Technology, and the Ministry of Health, Labor and Welfare.

Disclosure Information: The authors have nothing to declare.

References

- Goodarzi MO, Bryer-Ash M 2005 Metformin revisited: re-evaluation of its properties and role in the pharmacopoeia of modern antidiabetic agents. *Diabetes Obes Metab* 7:654–665
- Lord J, Wilkin T 2004 Metformin in polycystic ovary syndrome. *Curr Opin Obstet Gynecol* 16:481–486
- Bergheim I, Luyendyk JP, Steele C, Russell GK, Guo L, Roth RA, Arteel GE 2006 Metformin prevents endotoxin-induced liver injury after partial hepatectomy. *J Pharmacol Exp Ther* 316:1053–1061
- Isoda K, Young JL, Zirikli A, MacFarlane LA, Tsuboi N, Gerdes N, Schonbeck U, Libby P 2006 Metformin inhibits proinflammatory responses and nuclear factor- κ B in human vascular wall cells. *Arterioscler Thromb Vasc Biol* 26:611–617
- Lin HZ, Yang SQ, Chuckaree C, Kuhajda F, Ronnet G, Diehl AM 2000 Metformin reverses fatty liver disease in obese, leptin-deficient mice. *Nat Med* 6:998–1003
- Morin-Papunen L, Rautio K, Ruokonen A, Hedberg P, Puukka M, Tapanaianen JS 2003 Metformin reduces serum C-reactive protein levels in women with polycystic ovary syndrome. *J Clin Endocrinol Metab* 88:4649–4654
- Attia GR, Rainey WE, Carr BR 2001 Metformin directly inhibits androgen production in human thecal cells. *Fertil Steril* 76:517–524
- Mansfield R, Galea R, Brincat M, Hole D, Mason H 2003 Metformin has direct effects on human ovarian steroidogenesis. *Fertil Steril* 79:956–962
- Momoeda M, Taketani Y, Terakawa N, Hoshiai H, Tanaka K, Tsutsumi O, Osuga Y, Maruyama M, Harada T, Obata K, Hayashi K 2002 Is endometriosis really associated with pain? *Gynecol Obstet Invest* 54(Suppl 1):18–21
- Osuga Y, Koga K, Tsutsumi O, Yano T, Maruyama M, Kugu K, Momoeda M, Taketani Y 2002 Role of laparoscopy in the treatment of endometriosis-associated infertility. *Gynecol Obstet Invest* 53(Suppl 1):33–39
- Harada M, Osuga Y, Hirota Y, Koga K, Morimoto C, Hirata T, Yoshino O, Tsutsumi O, Yano T, Taketani Y 2005 Mechanical stretch stimulates interleukin-8 production in endometrial stromal cells: possible implications in endometrium-related events. *J Clin Endocrinol Metab* 90:1144–1148
- Hirota Y, Osuga Y, Hirota T, Harada M, Morimoto C, Yoshino O, Koga K, Yano T, Tsutsumi O, Taketani Y 2005 Activation of protease-activated receptor 2 stimulates proliferation and interleukin (IL)-6 and IL-8 secretion of endometriotic stromal cells. *Hum Reprod* 20:3547–3553
- Koga K, Osuga Y, Yoshino O, Hirota Y, Yano T, Tsutsumi O, Taketani Y 2005 Elevated interleukin-16 levels in the peritoneal fluid of women with endo-

metriosis may be a mechanism for inflammatory reactions associated with endometriosis. *Fertil Steril* 83:878–882

- Yoshino O, Osuga Y, Hirota Y, Koga K, Hirata T, Harada M, Morimoto C, Yano T, Nishii O, Tsutsumi O, Taketani Y 2004 Possible pathophysiological roles of mitogen-activated protein kinases (MAPKs) in endometriosis. *Am J Reprod Immunol* 52:306–311
- Yoshino O, Osuga Y, Koga K, Hirota Y, Hirata T, Ruimeng X, Na L, Yano T, Tsutsumi O, Taketani Y 2006 FR 167653, a p38 mitogen-activated protein kinase inhibitor, suppresses the development of endometriosis in a murine model. *J Reprod Immunol* 72:85–93
- D'Hooghe TM, Nugent NP, Cuneo S, Chai DC, Deer F, Debrock S, Kyama CM, Mihalyi A, Mwenda JM 2006 Recombinant human TNFRSF1A (rhTBP1) inhibits the development of endometriosis in baboons: a prospective, randomized, placebo- and drug-controlled study. *Biol Reprod* 74:131–136
- Dogan E, Saygili U, Posaci C, Tuna B, Caliskan S, Altunyurt S, Saati B 2004 Regression of endometrial explants in rats treated with the cyclooxygenase-2 inhibitor rofecoxib. *Fertil Steril* 82(Suppl 3):1115–1120
- Efstathiou JA, Sampson DA, Levine Z, Rohan RM, Zurakowski D, Folkman J, D'Amato RJ, Ruppnick MA 2005 Nonsteroidal antiinflammatory drugs differentially suppress endometriosis in a murine model. *Fertil Steril* 83:171–181
- Hirota Y, Osuga Y, Hirota T, Yoshino O, Koga K, Harada M, Morimoto C, Nose E, Yano T, Tsutsumi O, Taketani Y 2005 Possible involvement of thrombin/protease-activated receptor 1 system in the pathogenesis of endometriosis. *J Clin Endocrinol Metab* 90:3673–3679
- Morimoto C, Osuga Y, Yano T, Takemura Y, Harada M, Hirota T, Hirota Y, Yoshino O, Koga K, Kugu K, Taketani Y 2005 G α 12 as a possible cytoskeletal regulator in the development of endometriosis. *Hum Reprod* 20:3212–3218
- Takemura Y, Osuga Y, Yamauchi T, Kobayashi M, Harada M, Hirota T, Morimoto C, Hirota Y, Yoshino O, Koga K, Yano T, Kadovaki T, Taketani Y 2006 Expression of adiponectin receptors and its possible implication in the human endometrium. *Endocrinology* 147:3203–3210
- Zhou G, Myers R, Li Y, Chen Y, Shen X, Fenyk-Melody J, Wu M, Ventre J, Doebber T, Fujii N, Musi N, Hirshman MF, Goodyear LJ, Moller DE 2001 Role of AMP-activated protein kinase in mechanism of metformin action. *J Clin Invest* 108:1167–1174
- Pentikainen FJ, Neuvonen FJ, Penttilä A 1979 Pharmacokinetics of metformin after intravenous and oral administration to man. *Eur J Clin Pharmacol* 16:195–202
- Tucker GT, Casey C, Phillips PJ, Connor H, Ward JD, Woods HF 1981 Metformin kinetics in healthy subjects and in patients with diabetes mellitus. *Br J Clin Pharmacol* 12:235–246
- Nomura K, Murakami K, Shozu M, Nakama T, Yui N, Inoue M 2006 Local application of danazol-loaded hyaluronic acid hydrogel to endometriosis in a rat model. *Fertil Steril* 85(Suppl 1):1157–1167
- Ohno K, Araki N, Yamase T, Nawata H, Iida M 2004 A novel nonradioactive method for measuring aromatase activity using a human ovarian granulosa-like tumor cell line and an estrone ELISA. *Toxicol Sci* 82:443–450
- Ariel A 2002 Local cytokines in endometrial tissue: the role of interleukin-8 in the pathogenesis of endometriosis. *Ann NY Acad Sci* 955:101–109
- Attar E, Bulun SE 2006 Aromatase and other steroidogenic genes in endometriosis: translational aspects. *Hum Reprod Update* 12:49–56
- Akoum A, Lawson C, McColl S, Villeneuve M 2001 Ectopic endometrial cells express high concentrations of interleukin (IL)-8 in vivo regardless of the menstrual cycle phase and respond to oestradiol by up-regulating IL-1-induced IL-8 expression in vitro. *Mol Hum Reprod* 7:859–866
- Akoum A, Lemay A, Paradis I, Rheault N, Maheux R 1996 Secretion of interleukin-6 by human endometriotic cells and regulation by proinflammatory cytokines and sex steroids. *Hum Reprod* 11:2269–2275
- Gazvani MR, Christmas S, Quenby S, Kirwan J, Johnson PM, Kingsland CR 1998 Peritoneal fluid concentrations of interleukin-8 in women with endometriosis: relationship to stage of disease. *Hum Reprod* 13:1957–1961
- Iwabe T, Harada T, Tsudo T, Tanikawa M, Onohara Y, Terakawa N 1998 Pathogenetic significance of increased levels of interleukin-8 in the peritoneal fluid of patients with endometriosis. *Fertil Steril* 69:924–930
- Bruun JM, Pedersen SB, Richelsen B 2000 Interleukin-8 production in human adipose tissue. Inhibitory effects of anti-diabetic compounds, the thiazolidinedione ciglitazone and the biguanide metformin. *Horm Metab Res* 32:537–541
- Ailawadi RK, Jobanputra S, Kataria M, Gurnes B, Bulun SE 2004 Treatment of endometriosis and chronic pelvic pain with letrozole and norethindrone acetate: a pilot study. *Fertil Steril* 81:290–296
- Razzi S, Fava A, Sartini A, De Simone S, Cobellis L, Petraglia F 2004 Treat-

- ment of severe recurrent endometriosis with an aromatase inhibitor in a young ovariectomized woman. *BJOG* 111:182-184
36. Shippen ER, West Jr WJ 2004 Successful treatment of severe endometriosis in two premenopausal women with an aromatase inhibitor. *Fertil Steril* 81:1395-1398
 37. Soysal S, Soysal ME, Ozer S, Gul N, Gezgin T 2004 The effects of post-surgical administration of goserelin plus anastrozole compared to goserelin alone in patients with severe endometriosis: a prospective randomized trial. *Hum Reprod* 19:160-167
 38. Takayama K, Zeitoun K, Gunby RT, Sasano H, Carr BR, Bulun SE 1998 Treatment of severe postmenopausal endometriosis with an aromatase inhibitor. *Fertil Steril* 69:709-713
 39. Li L, Mamputu JC, Wiernsperger N, Renier G 2005 Signaling pathways involved in human vascular smooth muscle cell proliferation and matrix metalloproteinase-2 expression induced by leptin: inhibitory effect of metformin. *Diabetes* 54:2227-2234
 40. Session DR, Kalli KR, Tummon IS, Damario MA, Dumesic DA 2003 Treatment of atypical endometrial hyperplasia with an insulin-sensitizing agent. *Gynecol Endocrinol* 17:405-407
 41. Kola B, Boscaro M, Rutter GA, Grossman AB, Korbonits M 2006 Expanding role of AMPK in endocrinology. *Trends Endocrinol Metab* 17:205-215
 42. Takemura Y, Osuga Y, Harada M, Hirata T, Koga K, Yoshino O, Hirota Y, Morimoto C, Yano T, Taketani Y 2005 Concentration of adiponectin in peritoneal fluid is decreased in women with endometriosis. *Am J Reprod Immunol* 54:217-221
 43. Takemura Y, Osuga Y, Harada M, Hirata T, Koga K, Morimoto C, Hirota Y, Yoshino O, Yano T, Taketani Y 2005 Serum adiponectin concentrations are decreased in women with endometriosis. *Hum Reprod* 20:3510-3513
 44. Lebovic DI, Kir M, Casey CL 2004 Peroxisome proliferator-activated receptor- γ induces regression of endometrial explants in a rat model of endometriosis. *Fertil Steril* 82(Suppl 3):1008-1013
 45. Demirturk F, Aytan H, Caliskan AC, Aytan P, Koseoglu DR 2006 Effect of peroxisome proliferator-activated receptor-agonist rosiglitazone on the induction of endometriosis in an experimental rat model. *J Soc Gynecol Investig* 13:58-62
 46. Pritts EA, Zhao D, Ricke E, Waite L, Taylor RN 2002 PPAR- γ decreases endometrial stromal cell transcription and translation of RANTES *in vitro*. *J Clin Endocrinol Metab* 87:1841-1844
 47. Houston KD, Copland JA, Broadus RR, Gottardis MM, Fischer SM, Walker CL 2003 Inhibition of proliferation and estrogen receptor signaling by peroxisome proliferator-activated receptor ligands in uterine leiomyoma. *Cancer Res* 63:1221-1227
 48. Nisolle M, Donnez J 1997 Peritoneal endometriosis, ovarian endometriosis, and adenomyotic nodules of the rectovaginal septum are three different entities. *Fertil Steril* 68:585-596
 49. Wu Y, Kajdacsy-Balla A, Strawn E, Basir Z, Halverson G, Jaiwala P, Wang Y, Wang X, Ghosh S, Guo SW 2006 Transcriptional characterizations of differences between eutopic and ectopic endometrium. *Endocrinology* 147:232-246

JCEM is published monthly by The Endocrine Society (<http://www.endo-society.org>), the foremost professional society serving the endocrine community.

Interleukin (IL)-17A Stimulates IL-8 Secretion, Cyclooxygenase-2 Expression, and Cell Proliferation of Endometriotic Stromal Cells

Tetsuya Hirata, Yutaka Osuga, Kahori Hamasaki, Osamu Yoshino, Mika Ito, Akiko Hasegawa, Yuri Takemura, Yasushi Hirota, Emi Nose, Chieko Morimoto, Miyuki Harada, Kaori Koga, Toshiki Tajima, Shigeru Saito, Tetsu Yano, and Yuji Taketani

Department of Obstetrics and Gynecology (T.H., Y.O., K.H., O.Y., A.H., Y.Takem., Y.H., E.N., C.M., M.H., K.K., T.T., T.Y., Y.Taket.), Faculty of Medicine, University of Tokyo, Tokyo 113-8655, Japan; and Department of Obstetrics and Gynecology (M.I., S.S.), University of Toyama, Toyama 930-0194, Japan

IL-17A is secreted from Th17 cells, a discovery leading to revision of the mechanism underlying the role of Th1/Th2 in the immune response. Strong evidence suggests that immune responses associated with inflammation are involved in the pathogenesis of endometriosis. In the present study, we first demonstrated that the presence of Th17 cells in peritoneal fluid of endometriotic women by flow cytometric analysis and IL-17A-positive cells in endometriotic tissues by immunohistochemistry. To investigate the role of IL-17A in the development of endometriosis, we then studied the effect of IL-17A on IL-8 production, cyclooxygenase-2 expression, and cell pro-

liferation of cultured endometriotic stromal cells (ESCs). IL-17A enhanced IL-8 secretion from ESCs in a dose-dependent manner. The IL-17A-induced secretion of IL-8 from ESCs was suppressed by anti-IL-17 receptor A antibodies or inhibitors of p38 MAPK, p42/44 MAPK, and stress-activated protein kinase/c-Jun N-terminal kinase. Addition of TNF α synergistically increased IL-17A-induced IL-8 secretion from ESCs. IL-17A also enhanced the expression of cyclooxygenase-2 mRNA and proliferation of ESCs. IL-17A may play a role in the development of endometriosis by stimulating inflammatory responses and proliferation of ESCs. (*Endocrinology* 149: 1260–1267, 2008)

ENDOMETRIOSIS, DEFINED BY the presence of viable endometriotic tissue outside the uterus, is an enigmatic disease. Implantation and growth of endometrial cells from the overflow of menstrual blood into the peritoneal cavity is a widely accepted hypothesis for the pathogenesis of endometriosis. Although retrograde menstruation is observed in most women, only a fraction develop endometriosis. Multiple lines of evidence suggest that inflammation and immune responses play a pivotal role in the pathogenesis of endometriosis (1, 2).

Recent expeditious understanding of Th17 cells substantially revised the conventional Th1/Th2 hypothesis of T cell immunology (3–5). Th17 cells, along with Th1 and Th2 cells, differentiate from naïve T cells. Interferon- γ and IL-4 are specific cytokines secreted from Th1 and Th2 cells, respectively. IL-17A is a representative cytokine secreted from Th17 cells. IL-17A, a disulfide-linked homodimeric glycoprotein consisting of 155 amino acids, has been described in various immune responses and inflammation (6).

Elevated levels of inflammatory substances and cells in the peritoneal fluid (PF) of women with endometriosis is highly

indicative of pelvic cavity inflammation (7). A recent study demonstrated that increases in the level of IL-17A in PF correlate with the severity of endometriosis and infertility associated with this disorder (8).

In view of the emerging significance of IL-17A in a novel paradigm in immunology, we investigated the role of IL-17A in endometriosis. In the present study, we first examined presence of IL-17A immunoreactive cells in endometriotic tissues. In particular, we demonstrated Th17 cells in peritoneal fluid mononuclear cells (PFMCs). Thereafter, we studied effects of IL-17A on endometriotic stromal cells (ESCs). To this end, we mainly measured production of IL-8 in ESCs because IL-8 is a possible key player in endometriosis. It has been reported that IL-8 concentrations are increased in PF of endometriotic women, and IL-8 stimulates proliferation, matrix metalloproteinase activity, invasive capability, Fas ligand protein expression, and adhesion capability of endometrial stromal cells (9–11). We also examined cooperative effect of IL-17A to TNF α , another proinflammatory cytokine important for the disease (12). Finally, we studied direct proliferative effect of IL-17A on ESCs.

Materials and Methods

Reagents and materials

Human recombinant IL-17A, TNF α , goat antihuman IL-17A, goat IgG control, mouse antihuman IL-17 receptor (IL-17RA) and mouse IgG1 isotype control were purchased from R&D systems (Minneapolis, MN). Antibodies of human CD3, CD4, and mouse IgG1 isotype control and Goldstip were purchased from BD Bioscience (San Jose, CA). Antihuman IL-17A antibody and isotype control IgG1 were purchased from eBioscience (San Diego, CA). Antibodies of human p38 MAPK, phospho-

First Published Online December 13, 2007

Abbreviations: BrdU, 5-Bromo-2'-deoxyuridine; COX, cyclooxygenase; ESC, endometriotic stromal cell; FBS, fetal bovine serum; GAPDH, glyceraldehyde dehydrogenase; IL-17RA, antihuman IL-17 receptor; JNK, c-Jun N-terminal kinase; PF, peritoneal fluid; PFMC, PF mononuclear cell; PMA, phorbol 12-myristate 13-acetate; SAPK, stress-activated protein kinase.

Endocrinology is published monthly by The Endocrine Society (<http://www.endo-society.org>), the foremost professional society serving the endocrine community.

p38 MAPK, p42/44 MAPK, phospho p42/44 MAPK, stress-activated protein kinase (SAPK)/c-Jun N-terminal kinase (JNK), and phospho SAPK/JNK were purchased from Cell Signaling Technology (Beverly, MA). MAPK inhibitors SB202190, PD98059, and SP600125 were from Calbiochem (La Jolla, CA). Collagenase was obtained from WAKO (Osaka, Japan). The antibiotic mixture of penicillin, streptomycin, amphotericin B phorbol 12-myristate 13-acetate (PMA), and ionomycin were purchased from Sigma (St. Louis, MO). Charcoal-stripped fetal bovine serum (FBS) was from Hyclone (Logan, UT). DMEM/Ham's F12 (DMEM/F12) and deoxyribonuclease I were from Invitrogen (Rockville, MD).

Patients and samples

Endometriotic tissues and PF were obtained from patients with ovarian endometriomas undergoing laparoscopy. The severity of the disease was determined according to the revised American Society for Reproductive Medicine classification. The final diagnosis was confirmed by histopathological examination. Laparoscopic excision of ovarian endometrioma was performed as follows. After inspection of the pelvis, the ovary was freed from any adhesions. The cyst wall of endometrioma was stripped away from the normal ovarian tissue gently and completely. Endometriotic tissue were obtained from the excised cyst wall of ovarian endometrioma and transported to the laboratory in DMEM/F12 on ice under sterile condition. The PF was obtained from the patients, who were diagnosed as stage III or IV. All patients had regular menstrual cycles, and none had received hormonal treatment for at least 6 months before surgery. The tissues collected under sterile conditions were processed for the generation of primary cell cultures. The peritoneal fluid was collected under sterile conditions before any manipulative procedure. PFMCs were collected as previously described (13, 14). Briefly, the collected PF was centrifuged at $200 \times g$ for 5 min, and the supernatants were removed. The cell pellet was resuspended in PBS, layered onto Ficoll-Paque (Amersham Biosciences, Piscataway, NJ), and centrifuged at $150 \times g$ for 30 min. PFMCs were recovered from the interface.

The experimental procedures were approved by the Institutional Review Board of the University of Tokyo and signed informed consent for use of the endometriotic tissue was obtained from each patient.

Immunohistochemistry

Paraffin-embedded specimens were sliced at a 5- μ m thickness. These slide sections were deparaffinized and rehydrated. Antigens were retrieved by buffer at 98 C. Endogenous peroxidase was blocked by incubation for 20 min with a solution of 1% hydrogen peroxidase. Immunohistochemical tissue labeling was performed using the avidin-biotin peroxidase methods. After blocking with normal rabbit serum (Vector Laboratories, Burlingame, CA), the sections were incubated with 1 μ g/ml anti IL-17A antibody or goat IgG for 60 min at room temperature and incubated with avidin-biotin peroxidase complex (Vectastain Elite; Vector Laboratories), according to the manufacturer's instructions. The pattern of immunoreactivity was visualized using Vector VIP (Vector Laboratories) as substrate. All sections were counterstained with hematoxylin and evaluated under a light microscope.

Flow cytometric analysis

PFMCs were resuspended in 10% FBS RPMI 1640 medium. The cells were stimulated with PMA (50 ng/ml) and ionomycin (1 μ g/ml) for 5 h

in the presence of Goldstap. Cells were firstly stained extracellularly with anti-CD3 and anti-CD4 antibodies, then fixed and permeabilized with Perm/Fix solution (eBioscience), and finally stained intracellularly with anti-IL-17A antibody. Samples were analyzed using FACSCalibur (BD Bioscience) and Cell Quest Pro (BD Bioscience).

Isolation and culture of ESCs

The isolation and culture of human ESCs were performed as described previously (15, 16). Fresh endometriotic tissue collected in sterile medium was rinsed to remove blood cells. The tissue was minced into small pieces and incubated in phenol-red free DMEM/F12 containing type I collagenase (0.25%) and deoxyribonuclease I (15 IU/ml) for 120 min at 37 C. The resultant dispersed endometriotic cells were separated by filtration through a 100- μ m nylon cell strainer (Becton Dickinson and Co., Franklin Lakes, NJ) and 70 μ m nylon cell strainer. Stromal cells remaining in the filtrate were collected by centrifugation, resuspended in phenol-red free DMEM/F-12, plated onto 100-mm dishes (Iwaki, Asahi technology Co., Tokyo, Japan), and allowed to adhere at 37 C for 12 h. At the first passage, the cells were plated into six-well plates at 4×10^5 cells/well, 12-well plates at 2×10^5 cells/well, or 48-well plates at 1×10^5 cells/well. Once the cells reached confluence, in 2 or 3 d, they were used for experiments. The purity of ESCs was greater than 95%, according to positive cellular staining for vimentin and negative cellular staining for cytokeratin or CD45, CD68, and von Willebrand factor.

Treatment of the cells

First, to examine the effect of IL-17A on IL-8 production, the cells were incubated for 24 h in 5% FBS DMEM/F12 medium with varying doses of IL-17A. Second, to examine the effect of the anti-IL-17RA antibody, ESCs were preincubated in 5% FBS DMEM/F12 with the antibody for 30 min and then stimulated with 10 ng/ml IL-17A for 24 h. Third, to evaluate the effect of IL-17A on MAPK phosphorylation in ESCs, the cells were incubated with 5% FBS media with IL-17A (10 ng/ml) for different time periods. Fourth, to evaluate the effect of MAPK inhibitors, the cells were preincubated with each MAPK inhibitor for 1 h before the addition of IL-17A and then incubated for 24 h. Fifth, to evaluate the synergic effect of IL-17A and TNF α on IL-8 secretion, the cells were stimulated with varying doses of IL-17A (1–100 ng/ml) with or without TNF α (1 ng/ml). Finally, for time-course experiments examining the expression of IL-8 and cyclooxygenase (COX)-2 mRNA, ESCs were incubated with 5% FBS medium with IL-17A (10 ng/ml) for different time periods up to 24 h.

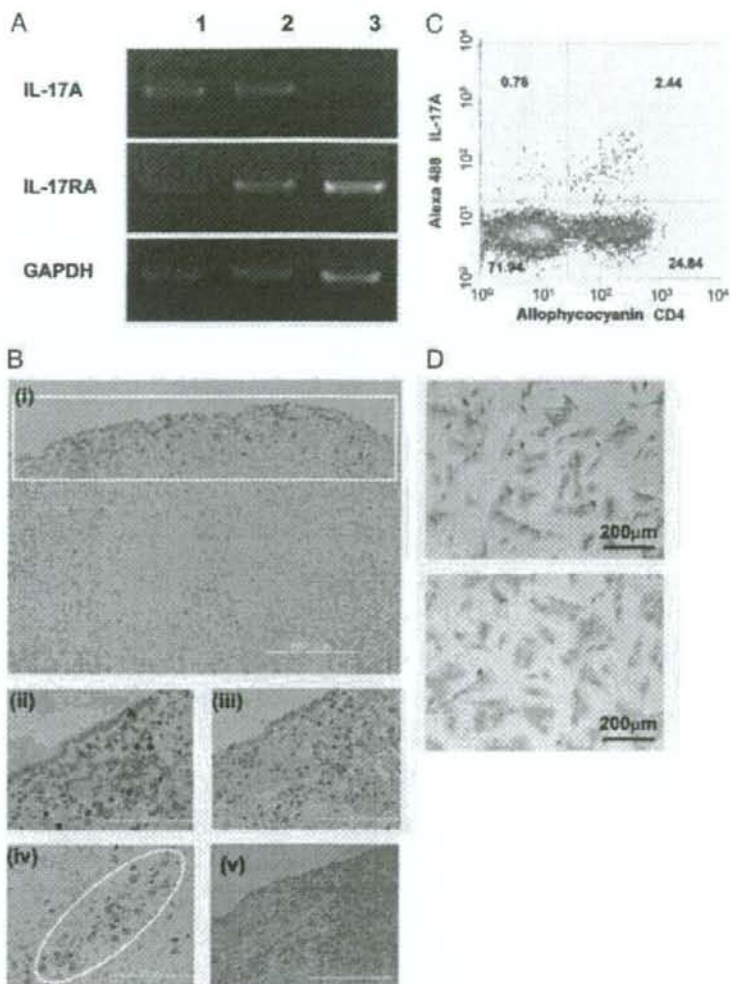
RNA extraction, reverse transcription, and PCR of IL-17A, IL-17RA, IL-8, and COX2

We extracted total RNA from endometriotic tissues and PFMCs by the acid guanidinium-phenol-chloroform method using ISOGEN (Nippongene, Toyama, Japan). Using an RNeasy minikit (QIAGEN, Hilden, Germany), we extracted total RNA from ESCs cultured in a 12-well plate. One microgram of total RNA was reverse transcribed in a 20- μ l vol using an RT-PCR kit (TOYOBO, Osaka, Japan). Standard PCR was performed using Rever Tra Dash (TOYOBO) according to the manufacturer's instructions. Human glyceraldehyde dehydrogenase (GAPDH) primers (TOYOBO) were used as a positive control for RNA levels. Primer pairs for IL-17A, IL-17RA, IL-8, and COX2 used in PCR are shown in Table

TABLE 1. Primer pairs used for PCR analysis

mRNA		Oligonucleotide sequences (5'–3')	Size (bp)
IL-17	Sense	ACTCCTGGGAAGACCTCATTGG	462
	Antisense	GGCCACATGGTGGACAATCG	
IL-17R	Sense	ACACCCAACAAGGAGACCTG	430
	Antisense	ATTCGTTCCACAGGGTGAAG	
IL-8	Sense	ACTTCCAAGCTGGCCGTGGCTCTCTGGCA	295
	Antisense	TGAATTCTCAGCCCTCTCAAAAATCTTC	
COX2	Sense	TTCAAATGAGATTGTGGGAAAATTGCT	306
	Antisense	AGATCATCTCTGCCTGAGTATCTT	
GAPDH	Sense	ACCACAGTCCATGCCATCAC	452
	Antisense	TCCACCACCCTGTGCTGTGA	

FIG. 1. A, Expression of IL-17A and IL-17RA mRNA in endometriotic tissues (lane 1), PFMCs (lane 2), and ESCs (lane 3). Endometriotic tissues, PFMCs, and ESCs without stimulation were analyzed by RT-PCR. B, Expression of IL-17A in the cyst wall of endometrioma (i, ii, iii, and iv) and ovary (v). Sections were immunostained with antihuman IL-17A antibody (i, ii, iv, and v) or goat IgG (iii). IL-17A-positive cells were detected in the stroma immediately beneath epithelium (i, white rectangular area). Arrowheads indicate IL-17A-positive cells in the stroma immediately beneath epithelium (ii). IL-17A-positive cells (arrowheads) were detected at the site of hemosiderin deposits (iv, white circle). No IL-17A-positive cells were detected in ovarian surface (v). Magnification, $\times 100$ (i), $\times 400$ (ii and iii), and $\times 200$ (iv and v). Scale bars, 200 μm (i, iv, and v); 100 μm (ii and iii). C, Th17 cells in PFMCs of patients with endometriosis. PFMCs were stimulated with PMA (50 ng/ml) and ionomycin (1 $\mu\text{g}/\text{ml}$) and labeled with an antibody specific to lymphocytes (CD3 and CD4) and IL-17A. Th17 cells were CD4 positive and IL-17A positive. The data shown are representative of four separate experiments. D, Immunocytochemistry of IL-17RA in ESCs. Cultured ESCs were immunostained with anti-IL-17RA antibody (upper photo). Lower photo shows the control with mouse IgG1 isotype. Magnification, $\times 100$.



1. PCR conditions for amplification were 30 cycles (for IL-17RA, IL-8, COX-2, and GAPDH) or 35 cycles (for IL-17A) at 98 C for 10 sec, 60 C for 2 sec, and 74 C for 14 sec. Each PCR product was purified with a QIAEX II gel extraction kit (QIAGEN), and the identity of PCR products was confirmed using an ABI PRISM 310 genetic analyzer (Applied Biosystems, Foster City, CA).

Real-time quantitative PCR

Real-time quantitative PCR was performed as reported previously (17). To assess IL-8 and COX2 mRNA expression, real-time quantitative PCR and data analysis were performed using Light Cycler (Roche Diagnostics GmbH, Mannheim, Germany). Expression of IL-8 and COX2 mRNA was normalized to RNA loading for each sample using GAPDH mRNA as an internal standard. The primers for IL-8 and COX2 were the same as those used for standard PCR. PCR conditions were as follows: for IL-8, 40 cycles at 95 C for 10 sec, 66 C for 10 sec, 72 C for 11 sec; for COX2, 30 cycles at 95 C for 10 sec, 66 C for 10 sec, 72 C for 13 sec; for GAPDH, 30 cycles at 95 C for 10 sec, 64 C for 10 sec, 72 C for 18 sec. All PCR conditions were followed by melting curve analysis.

Counting cell numbers

Cell counting was performed using a Cell Counting Kit-8 (Dojindo, Kumamoto, Japan), according to the manufacturer's instruction.

5-Bromo-2'-deoxyuridine (BrdU) incorporation assay

BrdU incorporation assay was performed as reported previously (15, 18, 19). The effects of IL-17A and IL-8 on the proliferation of ESCs was examined by measuring BrdU incorporation into DNA using the Biotrak cell proliferation ELISA system (Amersham Biosciences) according to the manufacturer's instructions. Briefly, ESCs were seeded into a 96-well plate (Becton Dickinson) at a density of 5×10^4 cells/well in 100 μl of the culture medium. After 24 h, cells were stimulated with IL-17A or IL-8 for 48 h. Then 10 μl BrdU solution were added and incubated at 37 C for an additional 2 h. After removing the culture medium, the cells were fixed and the DNA denatured by the fixative. The peroxidase-labeled anti-BrdU bound to the BrdU incorporated in the newly synthesized, cellular DNA. The immune complexes were detected by the subsequent substrate reaction, and the resultant color was read

at 450 nm in the DigiScan microscope reader (ASYS Hitech GmbH, Eugendorf, Austria).

Immunocytochemistry

ESCs were cultured in 16-well chamber slides (Nunc, Naperville, IL) in a humidified 5% CO₂-95% air environment and allowed to grow to approximately 50% confluence. The cells were fixed with cold methanol/acetone at -20°C for 20 min, washed twice with PBS, blocked for 20 min with 5% bovine serum in PBS, and incubated with an anti-IL-17RA antibody (10 µg/ml in 1.5% BSA in PBS) or IgG2b mouse IgG isotype control for 40 min at room temperature. After three washes with PBS, the slides were incubated with peroxidase-conjugated secondary antibody (goat antimouse Envision plus; Dako, Glostrup, Denmark) for 30 min at room temperature. Staining was detected with the diaminobenzidine chromogen after 3 min. All slides were counterstained with hematoxylin and evaluated under a light microscope.

Western blotting

Cultured cells in 6-well plates were homogenized in lysis buffer containing 50 mM Tris-HCl (pH 6.8), 2% sodium dodecyl sulfate, 10% glycerol, 50 mM dithiothreitol, and 0.1% bromophenol blue. The lysates were further diluted with lysis buffer to give a final concentration of 1 mg total protein per milliliter. Samples were resolved using 10% SDS-PAGE. Proteins were blotted onto a nitrocellulose membrane and incubated with rabbit antibodies to p38 MAPK (1:1000), phospho-specific p38 MAPK (1:1000), p42/44 MAPK (1:1000), phospho-specific p42/44 MAPK, SAPK/JNK (1:1000), phospho-specific SAPK/JNK (1:1000) as primary antibodies, and antirabbit horseradish peroxidase antibody (1:1000) as a secondary antibody. Immune complexes were visualized by use of the ECL Western blotting system (Amersham Biosciences).

Measurement of IL-8

The concentration of IL-8 in conditioned media was measured using a specific ELISA kit (Genzyme/Techno, Minneapolis, MN). The sensitivity of the assay was 15.6 pg/ml. The intraassay and interassay coefficients of variation were less than 5%.

Statistical analysis

Data were evaluated using ANOVA with Scheffé's *post hoc* analysis for multiple comparisons and Student's *t* test for two groups. *P* < 0.05 was accepted as statistically significant.

Results

Expression of IL-17A and IL-17RA mRNA in endometriotic tissue, PFMCs, and ESCs

The expression of IL-17A mRNA was detected in endometriotic tissues and peritoneal cells, but not in ESCs, by standard RT-PCR analysis. The expression of IL-17RA mRNA was detected in endometriotic tissues, PFMCs, and ESCs (Fig. 1A).

In vivo expression of IL-17A in the endometriotic lesion

As shown in Fig. 1B, the presence of immunoreactive IL-17A was detected in the cyst wall of endometrioma. Intense IL-17A immunoreactive cells were localized in the stroma immediately beneath epithelium and at the site of hemosiderin deposits. No IL-17A immunoreactivity was visualized in endometriotic epithelial cells. Few IL-17A-positive cells were observed in the endometrium of proliferative and secretory phases (data not shown). No IL-17A-positive cells were detected in ovarian surface. No staining was observed when normal goat IgG was used as a primary antibody.

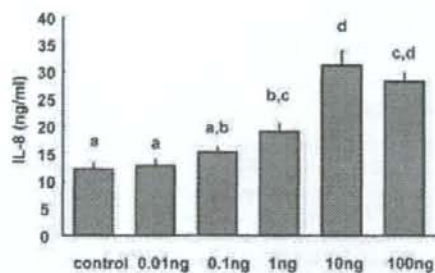


FIG. 2. IL-17A stimulates IL-8 secretion in ESCs. ESCs were cultured in 5% FBS with different doses of IL-17A for 24 h. Concentration of IL-8 in the conditioned medium was measured using a specific ELISA. Values are the mean \pm SEM of pentaplicate cultures. Different letters denote significant differences between groups (*P* < 0.05). The result is representative of nine separate experiments using samples from different patients.

Th17 cells in PFMCs of patients with endometriosis

The presence of IL-17A-producing cells was evaluated by flow cytometry on T cells (CD3+ cells) from PFMCs after stimulation with PMA and ionomycin. As shown in Fig. 1C, IL-17A-producing T cells were detected in PFMCs of patients with endometriosis. We also found IL-17A-producing T cells were predominantly CD4+ T cells.

Expression of IL-17RA protein in ESCs

The presence of immunoreactive IL-17RA was demonstrated in ESCs (Fig. 1D). No staining was observed when mouse IgG1 was used as a primary antibody.

Effects of IL-17A on IL-8 secretion by ESCs

As shown in Fig. 2, IL-17A at 1 ng/ml and higher significantly enhanced the secretion of IL-8 from ESCs. The maximum effect was observed with IL-17A at 10 ng/ml. The magnitude of increase

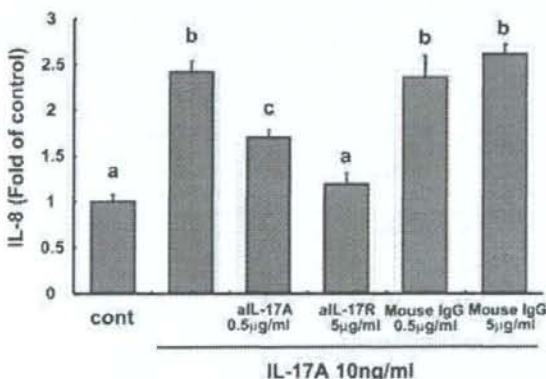


FIG. 3. Effect of anti-IL-17RA antibody (aIL-17R) on IL-17A-induced IL-8 secretion by ESCs. ESCs were preincubated in 5% FBS medium with or without mouse IgG1 and aIL-17R for 30 min and then stimulated with or without IL-17A (10 ng/ml) for 24 h. Concentrations of IL-8 in the conditioned media were measured using a specific ELISA. All values are expressed as the mean \pm SEM of pentaplicate cultures. Different letters denote significant differences between groups (*P* < 0.05). The result is representative of four separate experiments using samples from different patients. Cont, Control.

with 10 ng/ml IL-17A varied between patients from 1.8- and 5.3-fold, with a median increase of 3.5-fold ($n = 9$).

Effect of anti-IL-17RA antibody on IL-17A-induced IL-8 secretion in ESCs

Treatment with the neutralizing antibodies for IL-17RA significantly diminished the IL-17A-induced increase in IL-8 secretion in a dose-dependent manner, whereas the control IgG had no effect (Fig. 3).

Effect of IL-17A on MAPK phosphorylation in ESCs

The phosphorylation of three MAPKs (p42/44 MAPK, p38 MAPK, and SAPK/JNK) by IL-17A was determined in cultured ESCs (Fig. 4A). An increase in MAPK phosphorylation was apparent after 5–15 min. Phosphorylation levels reached a maximum after 5 min for P42/44 MAPK and after 15 min for p38 MAPK and SAPK/JNK, respectively.

Effect of MAPK inhibitors on IL-17A-induced IL-8 secretion

The intracellular mechanism of IL-17A-induced secretion of IL-8 by ESCs was investigated by examining the

effect of MAPK inhibitors. As shown in Fig. 4B, the addition of inhibitors for p38MAPK, p42/44 MAPK, and SAPK/JNK significantly diminished IL-17A-induced IL-8 secretion.

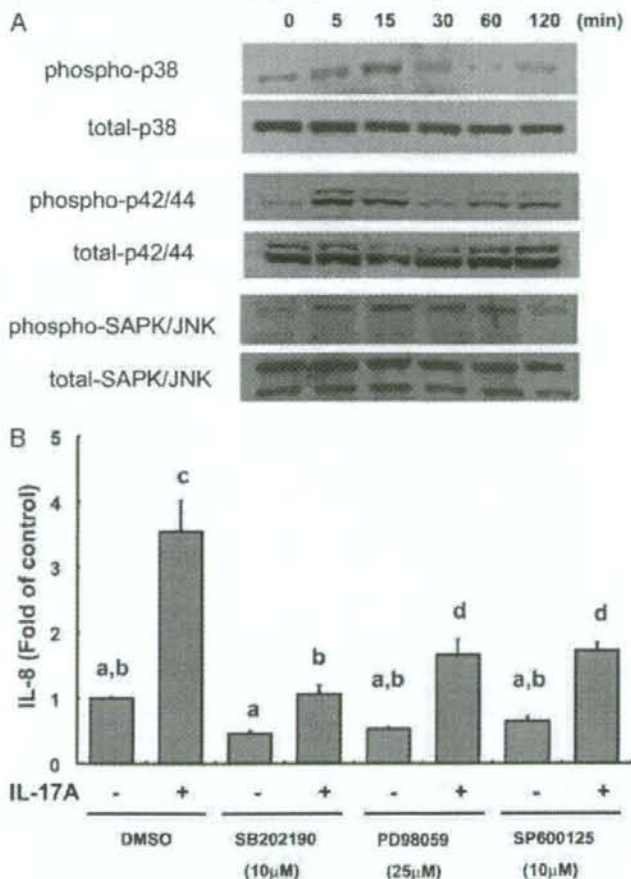
Synergistic effects IL-17A and TNF α on IL-8 secretion in ESCs

We chose TNF α as a representative proinflammatory cytokine known to induce IL-8 secretion from ESCs (12). TNF α together with IL-17A triggered IL-8 secretion above the combined levels generated by each stimulus alone (Fig. 5). This synergistic effect was apparent when TNF α (1 ng/ml) was combined with 1 ng/ml IL-17A, and maximal synergy was obtained at the highest dose of IL-17A tested (100 ng/ml).

Effect of IL-17A on the expression of IL-8 mRNA and COX2 mRNA in ESCs

Time-course experiments were conducted to examine the effect of IL-17A on the expression of IL-8 mRNA and COX2 mRNA in ESCs (Fig. 6A). Real-time quantitative PCR anal-

FIG. 4. Involvement of MAPKs in IL-17A induced IL-8 secretion from ESCs. A, Phosphorylation of p38 MAPK, p42/44 MAPK, and SAPK/JNK induced by IL-17A in ESCs. ESCs were incubated with IL-17A (10 ng/ml) for the indicated time (0–120 min). Cell lysates were assayed for phosphorylated p38 MAPK (phospho-p38), total p38 MAPK (total-p38), phosphorylated p42/44 MAPK (phospho-p42/44), total p42/44 (total-p42/44), phosphorylated SAPK/JNK (phospho-SAPK/JNK), and total SAPK/JNK (total-SAPK/JNK) by Western blotting. The data are representative of four independent experiments. B, Effects of MAPK inhibitors on IL-17A-induced IL-8 secretion in ESCs. ESCs were pretreated with or without inhibitors of p38 MAPK (SB202190), p42/44 MAPK (PD98059), and SAPK/JNK (SP600125) for 1 h and stimulated with IL-17A (10 ng/ml) for 24 h. The conditioned medium was collected and assayed for IL-8 concentration using a specific ELISA. All values are expressed as the mean \pm SEM of pentaplicate cultures. Different letters denote significant differences between groups ($P < 0.05$). The data are representative of four independent experiments. DMSO, Dimethylsulfoxide.



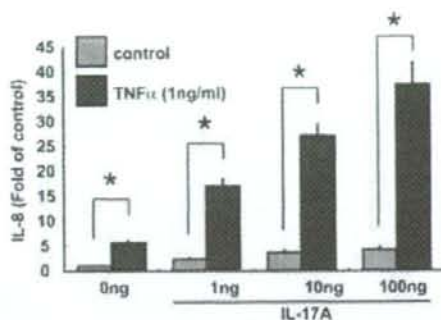


FIG. 5. Effect of IL-17A on TNF α -mediated IL-8 secretion from ESCs. ESCs were treated with IL-17A or TNF α or in combination for 24 h. The conditioned medium was collected and assayed for IL-8 concentration using a specific ELISA. All values are expressed as the mean \pm SEM of pentaplicate cultures. *, $P < 0.0001$ vs. each control. The data are representative of four independent experiments.

ysis demonstrated that IL-17A up-regulated IL-8 and COX2 mRNA. Maximal increases in IL-8 and COX2 mRNA were observed at 4 h, followed by a decrease with time up to 24 h (Fig. 6, B and C). The maximal increase of IL-8 mRNA was 6.2-fold of the control, and that of COX2 mRNA was 13.6-fold of the control.

Effect of IL-17A on cell proliferation of ESCs

The effect of IL-17A on cell proliferation was determined in ESCs (Fig. 7A). IL-17A at 10 and 100 ng/ml significantly increased cell number by 106 and 111%, respectively, after exposure for 48 h. As shown in Fig. 7B, IL-17A at 1–100 ng/ml significantly increased BrdU incorporation into DNA in ESCs. The maximal effect (3.98-fold of control) was observed at 10 ng/ml.

Discussion

In the present study, we first demonstrated that presence of IL-17A-positive cells in the endometriotic tissue. In addition, the presence of Th17 cells in PFMCs was clearly shown by flow cytometric analysis. These findings instigated us to examine possible roles of IL-17A in endometriosis. We then showed that IL-17A stimulated the secretion of IL-8 from ESCs. ESCs expressed IL-17RA, and the anti-IL-17RA antibody inhibited IL-17A-induced IL-8 secretion. IL-17A stimulated the activation of p38 MAPK, p42/44 MAPK, and SAPK/JNK, and inhibitors of these kinases suppressed IL-17A-induced IL-8 secretion. TNF α synergistically enhanced IL-17A-induced IL-8 secretion. IL-17A also stimulated ESC proliferation and COX2 expression in ESCs.

A recent study on the Th1/Th2 concept of T cell immunology revealed that endometriosis is an inflammatory disease with a Th2 immune response component (20, 21). The emerging concept of the Th17 pathway has challenged the conventional paradigm of Th1/Th2 hypothesis (4, 5). Together with the recent discovery of Treg, our understanding of the mechanisms underlying T cell immunology has advanced into a new era. In this context, the presence of Th17 cells in PFMCs demonstrated in our study might lead the

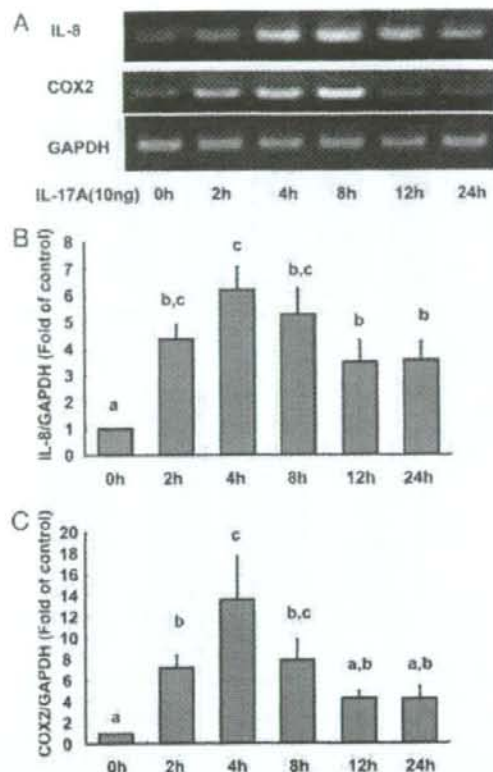


FIG. 6. Effect of IL-17A on the expression of IL-8 and COX2 mRNA in ESCs. ESCs were incubated with IL-17A (10 ng/ml) for the indicated duration. A, Expression of IL-8 and COX2 mRNA in ESCs was examined by RT-PCR. The data shown are representative of four separate experiments using samples from different women. B, Expression of IL-8 mRNA in ESCs was examined by real-time quantitative PCR. The data shown are the relative ratio (IL-8 to GAPDH) measured by real-time quantitative PCR. Data are the mean \pm SEM of five independent experiments using samples from five different women. Different letters denote significant differences between groups ($P < 0.05$). C, Expression of COX2 mRNA in ESCs was examined by real-time quantitative PCR. The data shown are the relative ratios (COX2 to GAPDH) measured by real-time quantitative PCR. Data are the mean \pm SEM of five independent experiments using samples from 5 different women. Different letters denote significant differences between groups ($P < 0.05$).

concept of immune response in endometriosis to a novel direction. In particular, abundant IL-17A-positive cells in the endometriotic tissue imply possible Th17 immune response therein. The present study has demonstrated multiple functions of IL-17A in ESCs. Given that IL-17A is a key effector molecule of Th17 cells, our findings form the foundation for understanding the etiology of endometriosis under the novel concept of T cell differentiation and regulation.

Substantial evidence points to IL-8 as a pivotal factor involved in the progression of endometriosis. IL-8 exerts pleiotropic functions, such as chemoattraction and activation of neutrophils, angiogenesis, stimulation of proliferation, and